Characterization of VOCs and their related atmospheric processes in a central China city during severe ozone pollution periods

Bowei Li[1], Steven Sai Hang Ho[2,3*], Sunling Gong[1,4*], Jingwei Ni[1], Huairui Li[1], Liyan Han[1], Yi Yang[1], Yijin Qi[1], Dongxu Zhao[1]

[1] *Langfang Academy of Eco Industrialization for Wisedom Environment, Langfang 065000, China*

[2] *Division of Atmospheric Sciences, Desert Research Institute, Reno, Nevada, USA*

[3] *Key Lab of Aerosol Chemistry & Physics, Institute of Earth Environment, Chinese Academy of Sciences, Xi'an 710061, China*

[4] *Center for Atmosphere Watch and Services of CMA, Chinese Academy of Meteorological Sciences, Beijing 100081, China*

*Correspondence to: Steven Sai Hang Ho (stevenho@hkpsrl.org) and Sunling Gong (gongsl@cma.gov.cn)

Revision on: December 08, 2018

Abstract

A five-month campaign (from May to September 2017) was conducted to characterize volatile organic compounds (VOCs) for the first time at four sites in Zhengzhou City, Henan Province, China, where ground level ozone (O_3) concentration shown an increasing trend in recent years. Canister samples were collected for measurement of fifty-seven VOCs, which, along with reactive nitrogen oxides (NOx), are the most important O_3 precursors. During the same period, O_3 and its precursor gases were monitored online simultaneously. The results indicated that the average mixing ratio of total quantified VOCs (Σ_{VOCs} = 28.8±22.1 ppbv) in Zhengzhou was lower than that in the other Chinese megacities, while alkyne was a higher proportion of Σ_{VOCs}. The abundances, compositions and ratios of typical VOCs showed clear spatial and temporal variations. Cluster analysis indicates that air masses from south of Zhengzhou were cleaner than from other directions. The molar ratio of VOCs to NO_x indicated that , in general, O_3 formation was more sensitive to VOCs than NO_x formation in Zhengzhou. The source apportionment was conducted with Positive Matrix Factorization (PMF), and it was found that vehicle exhaust, coal and biomass burning, and solvent usage were the major sources for ambient VOCs at all four sites. From Potential Source Contribution Function (PSCF) analysis, the strong emissions from coal+biomass burning and solvent usage were concentrated in southwest of Shanxi and Henan province. The results of this study gather scientific evidences on the pollution sources for Zhengzhou city, benefiting the Government to establish efficient environmental control measures particularly for O_3 pollution.

1. Introduction

Volatile organic compounds (VOCs) are diverse and reactive chemicals. Vehicle exhausts, fuel combustion and evaporation, and solvent usage are the known major anthropogenic sources of VOCs (Fujita et al., 1994; US EPA, 2000; Fujita, 2001; Borbon et al., 2002) . VOCs play a crucial role in the ground-level ozone (O_3) pollution (Haagen-Smit, 1952; Choek and Heuss, 1987), which has troubled many rapid economy-growth urban cities (Wang et al., 2017b; Nagashima et al., 2017). Many related studies are thus being conducted globally (Wei et al., 2014; Malley et al., 2015; Ou et

al., 2015). In China, the investigations on VOCs including source apportionment, measurement of emission profiles and interpretation of seasonal variations were mainly concentrated in Yangtze River Delta (YRD), Pearl River Delta (PRD) and Beijing-Tianjin (BJT) regions (An et al., 2014; Wang et al., 2014; Chen et al., 2014; Liu et al., 2016; Guo et al., 2017). Limited studies have been conducted in less developed or developing regions (i.e., southwestern and northwestern China) where prominently impacted by biomass burning and with high abundances of toxic and reactive compounds (Li et al., 2014; Li et al., 2017a).

Fifty-seven VOCs, including C_2 - C_{10} alkanes, alkenes, alkynes and aromatics, which greatly contribute to ambient O_3 formation, have been identified and are regularly monitored by Photochemical Assessment Monitoring Stations (PAMS) (US EPA, 1990; Oliver et al., 1996). Due to characteristic structure and reactivity of these compounds, their contributions in O_3 production varies (Carter, 1994); it has been reported that aromatics and alkenes were responsible for most of the weighted reactivity of VOCs (59.4% and 25.8%, respectively) in Pearl River Delta (PRD) region in China (Ou et al., 2015). Consequently, researchers have deduced that reductions of alkenes and aromatics are suitable targets for O_3 control (Wang et al., 2018). In addition, with the variations on energy structure, industrial construction and meteorological conditions (Shao et al., 2011; Wang et al., 2015), major emission sources of VOCs at each city are unique. In less developed cities of Heilongjiang and Anhui, biomass combustion had the highest contribution (40% and 36%, respectively) to the O_3 formation potentials due to high quantity of agricultural activities, while in the developed cities such as Shanghai, Beijing and Zhejiang, solvent usage has become a more important source (Wu and Xie, 2017). Therefore, identification on district emission sources of VOCs is necessary to provide scientific-based information for policy-makers who establish efficient strategies to alleviate O_3 pollution.

In addition to the factors discussed above, non-linear relationships between ambient VOCs, nitrogen oxide (NO_x) and O_3 production such that decreasing tropospheric O_3 is more complex than expected (Lin et al., 1998; Hidy and Blanchard, 2015; Li et al., 2018). Many modeling and field studies showed that photochemical O_3 production in several cities in China such as Guangzhou, Shanghai and Beijing with high levels of NO_x were highly sensitive to VOCs (Shao et al., 2009; Ou

69 et al., 2016; Gao et al., 2017). The sensitivity regime is always varied with time and geographical

70 locations (Luecken et al., 2018). The percentage of VOC-limited regime in North China Plain (NCP)

71 increased from 4% to 6% between 2005-2013, owing to the rapid increases of NO_x emissions (Jin

72 and Holloway, 2015).

73 Zhengzhou City is an important developing city in the mid-west of the Huanghe-Huaihe river

74 flood plain in China. As the capital city of Henan Province, it is densely populated with more than

75 seven million residents in 2010 (Geng et al., 2013). With the rapid growth of industrial activities, as

76 well as increased vehicle emissions and fuel combustion, air quality in Zhengzhou has deteriorated.

77 The Air quality index (AQI) for 65% of the days in 2013 exceeded the allowable limits of 100

78 established by the Air Quality Guideline (Chinese Ministry of Environmental Protection, 2012).

79 Particularly O_3 was the major pollutant in summer and over 50% of the days in 2015, the mixing

80 ratio of O_3 exceeded the Grade I standard (100 μg m^{-3}) of daily maximum average 8-hour (DMA8)

81 in Henan (Shen et al., 2017; Gong et al., 2017; Liu et al., 2018). As one of the major precursors of

82 O_3, the study on VOCs is of significance for Zhengzhou, since no related researches are published

83 in peer-reviewed literature. In this work, a comprehensive sampling campaign for VOCs

84 measurement and characterization has been conducted at four monitoring stations during the time

85 period of May - September 2017. The spatial and temporal variations in VOCs in Zhengzhou were

86 determined. The contributions of major emission sources were quantified, and the relationship

87 among O_3-VOCs-NO_x was discussed in details. The results and implications from this study can

88 provide useful guidance for policy-makers to alleviate ozone pollution in Zhengzhou, China.

89 **2. Observation and Methodology**

90 **2.1 Sampling site**

91 Based on the density of population distribution, locations of industrial facilities, and the

92 prevailing winds, four sites have been selected for sample collection: Jingkai community (JK;

93 113.73°E, 34.72°N), municipal environmental monitoring station (MEM; 113.61°E, 34.75°N),

94 Yinhang school (YH; 113.68°E, 34.80°N) and Gongshui company (GS; 113.57°E, 34.81°N), which

95 are located at the southeastern, southwestern, northeastern and northwestern of Zhengzhou,

96 respectively (Fig. 1). There is a main airport highway and heavy-traffic ring roads approximately

97 500 m west of JK. Furthermore, the site is at a distance of 2 km from an industrial area, which

98 involves packaging and printing plants, and material distribution factories. It is noteworthy that

99 there are three coal-fired power plants in the urban area of Zhengzhou city. One of the power plants

100 with the highest production was 1.6 km northwest of MEM, and MEM was surrounded by a main

101 road with four traffic lanes, the distance between the nearest traffic light and the sampling site was

102 just 200 m. Both the MEM and YH include a mix of commercial and condensed residential areas,

103 whereas the apartments around YH are more aged. The GS site is surrounded by several

104 manufacturing plants, including pharmaceuticals, materials, foods and machineries.

105 Ten dry days with no rainfall record were chosen in every month during the period of May -

106 September, 2017 consequently, to represent a typical air quality condition in a month. Grab samples

107 were collected minute using 3.2 L stainless-steel canisters (Entech Instrument, Inc., Simi Valley,

108 CA, USA), which were pre-cleaned with high purity nitrogen and pressurized to 20 psi. Two

109 samples, one collected at 07:00 with increasing of human activities and another one collected at

110 14:00 with well-mixed of ambient air, were obtained on each sampling day. A total of 400 samples

111 were collected in this study. The chemical analysis was accomplished within two weeks after the

112 collection of samples. Real-time data for trace gases, including SO_2, CO, NO_2/NO_x and O_3, and

113 synchronous meteorological data, such as temperature (T), relative humidity (RH), wind direction

114 (WD) and wind speed (WS), were recorded at each air monitoring station, the message of relevant

115 equipment are listed in Table S1.

116 **2.2 Chemical Analysis**

117 In this study, the measurement of VOCs was based on Compendium Method TO-15, which

118 was established by U.S. EPA (US EPA, 1999). Air in the canister was concentrated using

119 liquid-nitrogen at -160 °C in a cryogenic pre-concentrator (7100A, Entech Instrument, Inc.). Both

120 CO_2 and H_2O were removed from the transfer line. The air was then thermally desorbed at 120 °C

121 and transferred for analysis to a gas chromatography (GC, 7890A, Agilent Technologies, Santa

122 Clara, CA, USA) coupled with dual detectors, i.e. a mass spectrometric detector (MSD) and a flame

123 ionization detector (FID) (5977E, Agilent Technology). Dual columns were applied for the

124 simultaneous analysis of C_2 - C_{11} hydrocarbons. A PLOT column (15 m, internal diameter of 0.32

125 mm and film thickness of 3.0 μm) was connected to the FID for detection of C_2 - C_5 NMHCs,

126 whereas C_5 - C_{10} NMHCs, oxygenated VOCs (OVOCs) and halocarbons were separated using a

127 DB-624 column (30 m×0.25 mm inner diameter × 3.0 μm film thickness), which was connected to

128 the MSD. Target compounds were identified with retention time and mass spectra, and quantified

129 with multi-point calibration curve in this study. The standard gas of PAMS (1 ppm; Spectra Gases

130 Inc, NJ, USA) was used to construct the calibration curves for the 57 target VOCs, including 28

131 alkanes, 11 alkenes, acetylene and 17 aromatics. Detailed information on the target analyses

132 involved in this study and their corresponding linearity of calibration (R^2), measurement relative

133 standard deviation (RSD), method detection limit (MDL), maximum increment reactivity (MIR,

134 Carter, 2010) are presented in Table S2.

135 **2.3 Positive matrix factorization (PMF)**

136 The U.S. EPA PMF 5.0 software was used for source apportionment (Lau et al., 2010; Abeleira

137 et al., 2017; Xue et al., 2017). Due to the complex chemical reactions, the application of PMF in

138 VOCs has to be based on a couple of principles: eliminating species with mixing ratios below MDL

139 and excluding species with high reactivity, except for the source markers(Guo et al., 2011; Shao et

140 al., 2016). Finally, 31 VOC species and NO_2 were chosen for the source apportionment analysis.

141 In this study, PMF was performed with fifty base runs for each site, results with the minimum

142 Q value (a parameter used to express uncertainties of PMF results) were considered as optimum

143 solutions. In Table S3 the r^2 between observed values and predicted values of selected VOCs and

144 NO_2 are presented for the four sites, the r^2 for most species (>80%) were higher than 0.6,

145 compounds with $r^2<0.6$ were down weighted when determine factor sources.

146 During PMF analysis, bootstrap method was used to evaluate stability and uncertainty of the

147 base run solution, setting the minimum correlation coefficient r^2 at 0.6, 100 bootstrap runs were

148 performed, and the results were showing in Table S4, and acceptable results (>80%) were gained

149 for all the factors.

Three to nine factors were selected to initiate the running of PMF, the Q/Q(exp) for every site at fixed factor size were presented in Table S5. With the increase of factor number, the ratios Q/Q(exp) were declined due to additional factors. When the factor size changing from 3 to 4, 4 to 5, and 5 to 6, the decrement of Q/Q(exp) were larger (~18-25%), while the change was lower than 12% after factors increased to 7, combined with the field conditions, six factors were defined at each site.

2.4 Potential source contribution function (PSCF)

In this trajectory-based study, the probability of air clusters with source concentration higher than a certain value was estimated (Hopke et al., 1995). Briefly, the PSCF value in ij[th] grid was the ratio of the number of endpoints with higher source concentration relative to the total number of endpoints in ij[th] grid cell. The criterion value, equal to 75th percentile of the targeted source concentration in this study, was used to verdict whether the value was higher or not. The 48-hour back trajectories was calculated with Hybrid Single-Particle Lagrangian Integrated Trajectory (HYSPLIT) model. Because there are many grid cells with small values, which could result in high uncertainty, a weighting function (Wij) was introduced results (WPSCF) (Polissar et al., 1999). According to average values of end points in each cell, in this case, Wij was presented as below.

$$W_{ij} = \begin{cases} 1.0 & n_{ij} > 30 \\ 0.7 & 10 < n_{ij} \leq 30 \\ 0.42 & 5 < n_{ij} \leq 10 \\ 0.05 & n_{ij} \leq 5 \end{cases}$$

2.5 Estimation of the initial NO$_x$ and VOCs

With the assumption that chemical loss of NO$_x$ and VOCs were mainly due to their reactions with hydroxyl radical (•OH), the initial mixing ratio of NO$_x$ can be calculated with the equation as (Shiu et al., 2007; Shao et al., 2009):

$$[NO_x] = [NO_x]_0 \exp(-k \, [•OH] \, \Delta t) \qquad (1)$$

172 where k stands for the reaction rate between NO_x and •OH. In this study, k was set as the product of

173 the rate constant for NO_2+•OH multiplied by the observed average ratio of NO_2/NO_x during this

174 campaign.

175   The photochemical age (Δt) can be estimated from the ratio between two compounds, emitted

176 from a common source, but having different reaction rate with •OH. For this case, the

177 photochemical age clock was performed with ethylbenzene (E) and m,p-xylene (X) (Sun et al.,

178 2016).

179   $[•OH]\ \Delta t=1/(k_x-k_E)\ [\ln(X_0/E_0)-\ln(C_X/C_E)]$ (2)

180 which k_x and k_E represent their rate constants with •OH, C_X and C_E correspond to the observed

181 mixing ratios; X_0 and E_0 were their initial concentrations. The X_0/E_0 was estimated from the 5th

182 percentile of the observed ratios at 07:00 in this paper.

183   The initial mixing ratio of VOC was estimated with the same method as for NO_x (Shiu et al.,

184 2007):

185   $[VOC]_0=[VOC]_t \exp (k_i [•OH] \Delta t)$ (3)

186 where $[VOC]_t$ was the observed mixing ratio of ith species and k_i was the correspondent rate

187 constant with •OH.

188 **3 Results and discussions**

189 **3.1 Meteorological variations and Mixing ratios**

190   Meteorological conditions are important factors that impact both the compositions and levels of

191 VOCs. During the sampling period, the T varied from 15 to 38℃, RH varied from 38 to 100%

192 (Fig.S1), and the dominant winds were northwestern and southeastern (Fig. 2). The air clusters,

193 analyzed by HYSPLIT model, showed moderate differences in each month (Fig. 3). In May,

194 clusters arriving at Zhengzhou demonstrated longer paths, and included six clusters in total, while

195 in June, the length of clusters were shorter. However, the concentration levels and compositions of

196 VOCs were similar in the two months. In May, the largest cluster (27.2%) was passed over from

197 Yinchuan, a central city in northwest China, then crossing several non-capital cities (i.e., Yanan,

198   Yuncheng and Luoyang) in Shanxi and Sichuan provinces. Such a long-range transport of

199   pollutants has less impact on the air quality of Zhengzhou, as comparable level and similar

200   compositions of VOCs were obtained during the period of May - June. In June, August and

201   September, approximately half of the air trajectories originated from the areas of Henan province,

202   indicating the air pollutants in Zhengzhou were impacted by local factors.

203   The total concentrations of VOCs (Σ_{VOCs}) are presented in Table 1. The Σ_{VOCs} varied at the four

204   sites, where the highest Σ_{VOCs} and their compositions were not identical across the sampling months

205   as well. In May 2017, the highest Σ_{VOCs} was reported at JK (37.6 ± 22.6 ppbv), followed by GS

206   (31.7 ± 18.7 ppbv), YH (30.1 ± 16.4 ppbv) and MEM (29.1 ± 15.3 ppbv), while the Σ_{VOCs} values for

207   the month of June, July, August and September were found to be in the order of:

208   GS>JK>MEM>YH, MEM>GS>JK>YH, YH>MEM>JK>GS, and MEM> YH > GS >JK,

209   respectively. This can be attributed to numerous factors that will be explored later in the paper.

210   Besides the emission sources (to be discussed in Section 3.2), the impacts controlled by

211   meteorological conditions should not be ignored as well. For instance, the prevailing wind in May

212   was northwestern at GS and YH, while the southwestern wind was dominant at JK (Fig 4). The

213   transport of air pollutants from urban center and industrial plants should be resulted in the highest

214   level of Σ_{VOCs} at JK. In June 2017, the prevailing wind was southeastern at MEM, YH and GS (Fig.

215   4). The average wind speed at GS (0.74 ± 0.33 m s^{-1}) was lower than that at MEM (1.84 ± 0.94 m s^{-1})

216   and YH (0.97 ± 0.36 m s^{-1}) (Table 2), indicating poor dispersion conditions at GS. The air pollutants

217   emitted from MEM and YH were more liable resulting in a higher level of Σ_{VOCs} at GS in June. It

218   should be noted that, when Σ_{VOCs} at JK was higher than that of GS, the level at YH was higher than

219   that of MEM, and vice versa. Except for the discriminations between the pollution sources at every

220   site, there may be some other factors (e.g. horizontal and vertical air advection) contribute to it.

221   Due to the variations of the planet boundary layer (PBL) height, solar radiation and emission

222   sources, the concentrations of VOCs displayed obvious differences between morning and afternoon

223   time (07:00 LT and 14:00 LT in this study). Compared with morning period, the aromatic

224   compounds showed lower compositions at 14:00 LT (Fig. 5), because of the increased planet

225   boundary layer and the active photochemical reactions, while alkenes always peaked in the14:00

226 LT. According to the dataset, the increases in alkene compositions (~4.3% uplift) were mainly due

227 to higher contributions of isoprene (~1.4% at morning and 7.6% in the afternoon), which was

228 mainly emitted from biogenic sources and increased exponentially with ambient temperature

229 (Guenther et al., 1993;Guenther et al., 1995).

230 The average Σ_{VOCs} values in Zhengzhou (28.8±22.1 ppbv) were significantly lower than those

231 in Beijing (65.6 ppbv), Hangzhou (55.9 ppbv), Guangzhou (47.3 ppbv) and Nanjing (43.5 ppbv),

232 and higher than that in Wuhan (23.3±0.5ppbv) (Table 3). Factors, including population density,

233 industrial activity, fuel composition, local stringent regulations for environmental protection, terrain,

234 and weather are the potential reasons for the differences in VOCs concentrations in those cities.

235 With regard to the weight percentage of major groups (Table 3), the composition of alkanes was the

236 largest in all cities because of their longer lifetimes and widespread sources (Fig. 5), while the

237 composition of aromatics was lower than alkenes in these cities except for Guangzhou. It is well

238 known that aromatics mainly originate from solvent usage and vehicle exhaust in summer. The

239 large amount of shoemaking and shipbuilding industries involving large amounts of solvent usage

240 may be the main reason for the higher composition of aromatics in Guangzhou. In comparison with

241 other four cities, the composition of aromatics in Zhengzhou was the lowest probably due to its less

242 solvent-used manufacturers than in Guangzhou, Hangzhou and Nanjing, and less numbers of

243 vehicles than in Beijing. Alkyne contributes least to VOCs in cities listed in Table 3, with higher

244 level observed in Zhengzhou, where ranked second after Hangzhou. Alkyne typically originates

245 from combustion sources. Zhu et al. (2016) observed that the composition of alkyne in the

246 biomass-burning period could be double of that in the non-biomass burning period (Zhu et al.,

247 2016). As Henan is the largest agricultural province in China and the sampling duration covered the

248 crop harvest season, the residents often used crop residues as the biofuel for their subsistence and a

249 higher alkyne composition in Zhengzhou was thus resulted.

250 **3.2 Temporal variations**

251 The time series of mixing ratios of NO_x, O_3 and Σ_{VOCs} at every site are shown in Fig. 6. The

252 results showed a distinctive temporal characteristic where lower levels of SO_2, CO, NO_x, O_3 and Σ

253 $_{VOCs}$ were observed in July and August (mid-summer) (Table S6). These results were similar to

254 those obtained for other urban areas worldwide (Cheng et al., 1997; Na et al., 2001; Li and Wang,

255 2012). Changes in PBL height, human activities, and abundance of •OH were the potential causes

256 for the phenomenon. The occurrence of precipitation, which is usually accompanied with better air

257 dispersion conditions, is also frequent in most areas of China during summer, resulting in

258 decreasing background level of air pollutants. Additionally, a series of effective local policies, such

259 as prohibition of painting and coating in open air and limitations on fuel supply between 10:00

260 -17:00 LT during hot summer days assisted in suppressing the emissions of VOCs. Meanwhile,

261 many organizations, such as schools, institutes and scattered private workshops, were closed due to

262 summer vacations. Some large-scale industries also stopped manufacturing processes for two weeks

263 during this period. Consequently, the anthropogenic emissions were reduced, which in turn resulted

264 in a decrease in VOCs, SO_2, and NO_x emissions. The reduction of precursor levels and unfavorable

265 photochemical conditions (such as, higher RH) resulted in the lower O_3 levels in July and August.

266 Beside local emissions, the long-range air mass also had some impacts on relatively lower

267 level of Σ_{VOCs} in July. As illustrated in Fig.3, different from other months, the air current was

268 originated with the largest portion (*ca*. 88.7%) of clusters from Hubei province, where the average

269 Σ_{VOCs} in its capital city (23.3±0.6 ppbv) (Lyu et al., 2016) was lower than that in Zhengzhou

270 (29.2±23.1ppbv). In combination with the lower weight percentage of photochemically-reactive

271 aromatics (10.3±4.2%), and the lowest toluene to benzene (T/B) ratio of 1.15±0.99 around this

272 period, it is possible that the cleaner air mass clusters originating from Hubei also contributed to the

273 reduction of Σ_{VOCs} in July.

274 As demonstrated in Fig. 6, the observed Σ_{VOCs} values at 07:00 LT were often higher than those

275 at 14:00 LT. The accumulation of pollutants during night-time and the temperature inversion in the

276 morning were the most reasonable explanations for this phenomenon. Stronger photochemical

277 reaction during noon-time led to the reduction in atmospheric VOCs. It should be noted that

278 pronounced Σ_{VOCs} were occasionally observed at MEM and GS (Fig. 7), which were potentially

279 ascribed to sharp changes in local emissions and meteorological conditions. Specifically, at MEM,

280 the distinctive increment was always accompanied with obvious increases of alkanes or aromatics

281 (Fig. 7). Since the T and RH were often consistent during the sampling period, the direct gas

evaporations should be constant as well. Therefore, the simultaneous increased concentrations of SO_2, CO and NO_x could illustrate the potential impacts from combustion sources, such as emissions from nearby thermal power plant. At GS, the increase of Σ_{VOCs} in June was usually with extremely high levels of aromatics, due to the disturbance from solvent use for building renovation during this period, and the abnormal high levels of Σ_{VOCs} in other months were related to the rising concentrations of C_3-C_4 alkanes, which were mainly originated from consumptions of compressed natural gas (CNG) or LPG (Huang et al., 2015). The results support the possible impact from a gas-fueled power plant located about 1 km southwest of the site (~18% of prevailing western wind at GS during May to September).

It is of interest to note that on the morning of 5th September, acetylene was found in extremely high concentrations (14.7 - 39.4 ppbv). Its mixing ratio in most of the urban areas was <10 ppbv (Duan et al., 2008; Guo et al., 2012; Louie et al., 2013). 5th September is a festival day for the people who worship their ancestors. A large number of incenses and offerings, made up of wood and paper, were burnt during the festival, resulting in an elevation of acetylene all over the Zhengzhou city (Zhu et al., 2016).

3.3 Spatial variations

The C_2 - C_5 alkanes, acetylene, ethylene, toluene and benzene were the most abundant VOCs detected at all sites (Fig.8), and the mixing ratios of toluene varied within a wide range at each site, because of its universal emission sources (e.g., vehicle exhaust emissions and solvent usage) (Barletta et al., 2005; Wang et al., 2014). These chemicals contributed >60% for Σ_{VOCs} at each site, illustrating strong combustion-related sources in Zhengzhou.

Among the four major organic classes, alkane was the most abundant group as a result of its widespread sources and longevity (Fig.5), accounted for 52.9%, 62.5%, 53.4%, 53.4% of the total Σ_{VOCs} at JK, MEM, GS, and YH, respectively. The highest composition of alkane was observed at MEM due to the stronger contributions of ethane, iso-pentane, and C_6-C_8 branched alkanes (Fig. S3), which are emitted from light-duty gasoline vehicles (Wang et al., 2017a).

308   The average Σ_{VOCs} were slightly higher at industrially impacted sites of GS (31.7±28.7 ppbv)

309   and JK (28.6±22.0 ppbv) than those at MEM and YH (Fig.9). Additionally, the air pollutants

310   related to the combustion processes, such as SO_2 and CO, were marginally more abundant, in

311   western areas of Zhengzhou (GS and MEM) (Fig.9). Under high levels of VOCs and sufficient

312   supply of NO_x, the highest average mixing ratio of O_3 was observed at GS, followed by YH where

313   even with, which had the lowest VOCs and NO_x, indicating that there are multiple factors, rather

314   than the absolute concentrations, contributing to the formation of the secondary pollutant, O_3 at

315   YH.

316   In June, the O_3 concentration often exceeded the national standard level of 80 ppbv, i.e., there

317   was severe air pollution during this period. The average mixing ratio of O_3 during daytime

318   (07:00-18:00 LT) in June, 2017 at JK, MEM, YH, and GS were 74.9±39.6 ppbv, 73.5±40.6 ppbv,

319   73.8±35.7 ppbv, and 88.0±46.1 ppbv, respectively (Table 4). The higher level of O_3 at GS was

320   accompanied with the higher Σ_{VOCs} (39.3±25.4ppbv). The weight percentage of aromatics (15.6±

321   12.1%) at GS was higher than those at other sites as well, indicating that the painting and other

322   renovation activities at GS was potentially an important factor for its high O_3 level in June. Even

323   though both the Σ_{VOCs} and specifically high O_3 formation potential compounds (such as alkenes and

324   aromatics) at MEM were slightly higher than those at YH (Table 4), the O_3 concentration at MEM

325   was not higher. This could be attributed to other critical precursors such as NO. NO at MEM

326   (7.72ppbv) was significantly higher than that at YH (2.57 ppbv) during daytime, indicating that the

327   titration reaction between O_3 and NO was more efficient at MEM.

328   Because photochemistry producing O_3 occurs over several hours to days, O_3 episodes are

329   attributable not only to local sources but also to regional transports. For example, Streets et al.

330   (2007) reported that with continuous southern winds, the O_3 level in Beijing was 20-30%

331   contributed from its neighboring cities in Hebei. During our study, a typical regional ozone

332   pollution was happened on August 10th at YH (Fig.6). On that day, the ratios of Σ_{VOCs}/NO_x at the

333   four sites were all less than 6.5 (ppbC/ppbv) (Fig. S4), indicating a regional VOC-control system,

334   and that VOCs are the critical contributors to the formation of O_3 in Zhengzhou. The reductions in

335   Σ_{VOCs} in the afternoons (around 14:00 LT) compared to mornings (around 07:00 LT) may have

336 been due, in part, to chemical loss of VOC as O_3 is formed. The reduction of Σ_{VOCs} and active

337 compounds (i.e., aromatic+alkene) at 14:00 relative to 07:00, 35% and 56% respectively, was least

338 at YH among the four sites (Fig. S4). Based on the wind direction, between 08:00 - 15:00 LT on

339 August 10th, YH was downwind of the other three sites (Fig. S4). All of this confirms that the

340 abnormally high O_3 at YH was caused by the transport of air pollutants from other sites on that day.

341 **3.4 VOCs/NOx ratio**

342 The VOCs/NO_x ratio is often used to distinguish whether a region is VOCs or NO_x limited in

343 O_3 formation. Generally, VOC-sensitive regimes occur when, with VOCs/NO_x ratios are lower than

344 10 in the morning; NO_x-sensitive regimes occur when VOCs/NO_x ratios are greater than 20 (Hanna

345 et al., 1996;Sillman, 1999). In this study, the mean value of VOCs/NO_x (ppbC/ppbv) were below 5

346 at all four sites (Fig.10), and 75% of the data points were < 6, indicating that the O_3 formation was

347 sensitive to VOCs in Zhengzhou, and the reductions on the emissions of VOCs will be a benefit for

348 O_3 alleviation.

349 The VOCs /NO_x showed differences among the four sites (Fig. 10), with the lowest value at

350 MEM (~3.8) and the highest value at JK (~4.7). The production of O_3 at MEM is more sensitive to

351 VOCs than at JK due to presence of strong NOx emissions from a thermal-power plant.

352 Approximately 14% of the measured VOCs /NO_x ratios of >8.0 were found in the NO_x-limited site

353 of JK, resulting from higher VOCs or lower NO_x emissions than at other sites. Both of the mixing

354 ratios and the statistical data showed higher levels of VOCs (with lower NO_x) at GS, where only ~4%

355 of the ratios of > 8 was observed, indicating that there must be other factors (unresolved in this

356 study) impacted the variation of O_3 formation regimes.

357 From the daily variations of VOCs /NO_x ratios (Fig. 10), higher values were observed at 14:00

358 LT than at 07:00 LT at all four sites, well correlated with less vehicle emissions or more

359 consumption paths for NO_x with stronger light intensity. The increment of VOCs /NO_x at 14:00 LT

360 was more obvious at JK and GS, suggesting that more emission sources of VOCs at daytime, and

361 resulting the O_3 formation system shifting to the transition area in the afternoon.

362   O$_3$ formation depends not only on the abundances of precursors (mainly VOCs and NO$_x$) but

363   also VOCs to NO$_x$ ratio (Sillman, 1999; Pollack et al., 2013). In this research, the mixing ratio of

364   O$_3$ at 14:00 LT presented a slightly positive trend (p<0.05) with the uplift of VOCs /NO$_x$ at JK (Fig.

365   11), consistent to the results observed at the megacity of Shanghai (Gao et al., 2017), where the O$_3$

366   formation was more sensitive to NO$_x$ when high O$_3$ levels were observed. Without considering the

367   advection of air parcels, this can be attributed to the increased O$_3$ production efficiency at high

368   VOCs /NO$_x$. There were no discernible trends at other sites, possibly due to the counteraction

369   imposed by other uncertain factors.

370   **3.5 Ratios of specific compounds**

371   Ratios of specific VOCs are useful to identify emission sources (Ho et al., 2009; Liu et al.,

372   2015; Raysoni et al., 2017). In order to characterize the differences in the contribution of various

373   sources at each site, ratios of i-pentane/n-pentane and toluene/benzene (T/B) ratios are discussed

374   here.

375   The ratio of i-pentane to n-pentane can be used to differentiate potential sources such as

376   consumption of natural gas, vehicle emissions and fuel evaporations. In areas heavily impacted by

377   natural gas drilling, the ratios lie in the range of 0.82 - 0.89 (Gilman et al., 2013; Abeleira et al.,

378   2017). Higher values are often reported for automobiles: in a range of 2.2 - 3.8 for vehicle

379   emissions; and 1.8 - 4.6 for fuel evaporation (McGaughey et al., 2004; Jobson et al., 2004; Russo et

380   al., 2010; Wang et al., 2013), whereas the ratios below unity was found for coal combustion (0.56 -

381   0.80) (Yan et al., 2017).

382   In this study, i-pentane and n-pentane were highly correlated (R^2=0.87 - 0.94) throughout the

383   whole sampling campaign (Fig. 12), indicating constant pollution sources for these two compounds.

384   The highest ratio of i/n-pentane was found at JK (2.59±0.45), which was comparable to the value

385   of 2.93 reported in a Pearl River Tunnel (Liu et al., 2008), thus indicating strong impacts from

386   traffic-related sources. The average ratio at MEM was 2.31±0.68, higher than the character ratios

387   of coal combustion, reasonably due to the observation site presented at upwind position of the

388   thermal power plant. And frequent idling may cover up the contribution from coal combustion,

389 reflecting the impact of traffic emissions. The average ratios at YH (1.94±0.57) and GS (1.63±

390 0.51) were lower than those at the above two sites, suggesting the comparatively stronger

391 contribution from coal burning.

392 Tunnel and roadside researches indicates that T/B ratio varies within the range of 1 - 2 when

393 the atmosphere is heavily impacted by vehicle emissions (Wang et al., 2002; Tang et al., 2007;

394 Gentner et al., 2013; Huang et al., 2015). The ratio of <0.6 was ascribed to other sources such as

395 coal combustion and biomass burning (Tsai et al., 2003; Akagi et al., 2011). The industrial activity

396 would be more dominant when the T/B ratio is greater than 3 (Zhang et al., 2015).

397 In this study, the correlation between benzene and toluene was fairly well at all the sites

398 (R^2=0.70-0.74), except for YH (R^2=0.41) (Fig.14), suggesting the similar sources for benzene and

399 toluene at JK, MEM and GS, while more complex such as variable wind direction at YH. The

400 average ratios of T/B were lied within the range of 1.64-2.29, which were scattered around the

401 character ratio of 2 for vehicle exhaust, illustrating the significance of vehicle emissions at the four

402 sites. Specifically, at JK, MEM and YH, most of T/B ratios were distributed between 0.6 and 3,

403 which were corresponding to character ratios for coal or biomass burning and industrial activities

404 respectively. These reflected the mixture impacts from mobile source and coal/biomass burning at

405 these three sites. However, more values were greater than 3 at GS, suggesting more frequent

406 disturbance from industrial activities at this site.

407 The T/B ratios at 14:00 LT were lower than at 07:00 LT (Fig.15). The reaction rate constant

408 of toluene ($5.63 \times 10^{-12} cm^3 molecule^{-1} s^{-1}$) with •OH is higher than that for benzene ($1.22 \times$

409 $10^{-12} cm^3 molecule^{-1} s^{-1}$), indicating more rapid consumption of toluene from photochemical reactions

410 and thus resulting in lower T/B ratios at 14:00 LT, all else being equal. The emission strength of

411 mobile source is often weaker at 14:00 LT, while the coal/biomass burning are increased due to

412 more human activities. Both chemistry and emissions offer an explanation of the lower T/B ratios

413 observed at 14:00 LT. In comparison with other months, higher T/B ratios were found more

414 frequently in September, potentially showing increased industrial activities during this period.

Overall, based on the iso-pentane/i-pentane and T/B ratios, the atmospheric VOCs at every site were impacted by a mix of coal/biomass burning and vehicle emissions, whereas GS was more liable impacted by industry-related sources.

3.6 Relative reactivity of VOCs

The reactivity of individual species is different, and in mixtures of VOCs there is competition for reaction partners, leading to variations in reaction pathways and O_3 formation yields. Ozone formation potential (OFP) is a useful tool to estimate maximum O_3 productions of each compound under optimum conditions, from which the most important species for O_3 formation could be identified (Carter, 1994). The calculation of OFP is based on mixing ratios and maximum incremental reactivity (MIR) of each individual compound, Eq. (4).

$$OFP=C_i \times MIR \qquad (4)$$

where C_i represents the concentration level of ith species, while *MIR* is a constant taken from (Carter, 2010) (Table S2).

In Zhengzhou city, alkenes contribute most ($55.9\pm14.2\%$) to the sum of OFP, of which ethylene had the largest portion. The results is different with the estimation based on emission inventories by Wu and Xie (2017), in which the largest contributor of total OFP in North China Plain (NCP), YRD and PRD was aromatics, reflecting that there was relatively less surface coating industries in Zhengzhou.

For the individual species, the top 10 most contributors in OFP included ethylene, isoprene, m,p-xylene, toluene , propylene, acetylene, n-butane, i-pentane and propane. Their contributions to the sum of OFP was lied within the range of 69.4 - 77.6% (Table 5), with 61.3-76.5% of total VOCs weighted in concentration, highlighting the importance of reduction on emissions of these VOCs no matter based on relative reactivity or mixing ratios. Additionally, it is worth noting that, the percentage of acetylene ($4.51\pm0.34\%$) weighted in OFP was higher than many other areas in China, including Guangzhou (2.20%) and YRD (2.37%) (Li and Wang, 2012; Jia et al., 2016), demonstrating that it is necessary to conduct emission controls on sources related to combustion (i.e., vehicle emissions and biofuel burning) in Zhengzhou city.

442   Zhengzhou was suffered from the severest O_3 pollution in June, 2017. The relationships

443   between OFP of each organic group, Σ_{VOCs}, and the ambient concentrations of NO_x and O_3, as well

444   as the corresponding meteorological conditions, are shown in Fig. S5-6. At 07:00 LT, generally

445   lower WS was seen than that at 14:00 LT, offered a favorite condition for local O_3 propagation.

446   Under low RHs and high T and OFP (88.1±30.3 ppbv), the O_3 level at YH was unexpectedly lower

447   than that at MEM on sunny days. Since the OFP was estimated with the assumption of reactions

448   that proceeded under optimum conditions, the above phenomenon reflected there were unsatisfied

449   O_3 formation conditions at YH. The highest total OFP was seen at JK in June, while the highest O_3

450   levels was observed at GS where located at a downwind position with lowest WS (0.74±0.33 m s^{-1}).

451   The concentration level of O_3 usually increased with wind speed (Fig.S7), particularly when the

452   eastern wind was dominant, illustrating the disturbance from long-distance sources to urban center.

3.7 Source apportionment

454   The factor profiles given by PMF for each site were presented in Fig.15. The six factors were

455   resolved as vehicle emissions, coal+biomass burning, solvent use, oil evaporation, petrochemical

456   and biogenic source (detailed characterization can be referred to supporting information) on the

457   base of the correspondent markers for each source categories, which were summarized in Table S7.

458   Meanwhile, the correlation coefficients, expressed in Pearson's r, were varied from 0.54 to 0.62

459   and 0.66 to 0.73 for SO_2 with coal+biomass burning, and NO_2 with vehicle emission, respectively

460   (Fig. 16), proved the precise results gained in this study.

461   The weight percentage of each factor calculated with two criteria (absolute concentrations and

462   OFPs) at the four sites were presented in Fig.17. At every site, vehicle emission, coal+biomass

463   burning and solvent use were the top three contributors to VOCs abundance in ambient air.

464   Compared to JK and YH, even though the distances between thermal power plant and the

465   observation site was the shortest at MEM, vehicle emission (36.8%) showed the largest portion

466   instead. Coal+biomass burning (30.6%) had the highest contribution at GS, attributed to its

467   downwind position and nearby suburbs that biomass burning occurred more frequently. The

468   contributions from vehicle emission at the two urban centers of MEM (36.8%) and YH (37.4%)

469   were comparable, but higher than those at JK and YH. The consumptions of solvent at GS (18.9%)

and JK (14.9%) were higher than those at YH (10.1%) and MEM (11.5%), due to restriction on development of new industrial enterprises in urban center in recent years. Emissions from oil evaporation, petrochemical and biogenic emission were scarce, and their contributions were below 10% at every site.

On the base of O_3 formation impact, coal+biomass burning, solvent use, and vehicle emission were the three major contributors as well. In contrast to the concentration weighted method, the importance of solvent use estimated with OFP increased 28-65% for each site, and the significance of vehicle emissions decreased 29-53%. At YH and GS, small discrimination (<4%) in contributions of coal+biomass burning between the two methods were found. On the other hand, the variations on coal+biomass burning at JK (a decline of 17%) and MEM (an increase of 29%) were more obvious, due to low abundance of reactive species in this factor at JK and high level of alkenes at MEM. Considering that the aging index of xylene/ethylbenzene was high at MEM (2.97) and low at JK (0.01) remarkably, demonstrating that the emission sources related to coal+biomass burning was fresher at MEM than JK.

Except for oil gas evaporation and biogenic sources, in which major emitted compounds with shorter life span, potential source regions for the other four identified sources (i.e., coal+biomass burning, vehicle emission, solvent usage and petrochemical) apportioned by PSCF method were presented in Fig. 18. Southwest of Shanxi province, western of Shandong province, and southwest of Henan province were identified as hot spots for the coal+biomass burning. The active emission areas for solvent use were concentrated in Henan province, and mainly located in southwest of Zhengzhou. The most contribution area for petrochemical was found in southwest of both Shanxi and Henan, northwest of Anhui, and southeast of Hubei provinces. For vehicle emissions, the strongest emission point was scattered in southwest of Henan, while Shandong, Anhui and Hubei provinces also distributed with strong emission points.

3.8 Consumption of VOCs and correlations with ozone level

The consumption of a VOC in the atmosphere could be presented as the difference from its initial mixing ratio and the observed value following an air parcel. In isolated stagnant air, the rate

of change of VOC concentrations will be the sum of emissions, deposition, and chemical production and loss processes.

The average value of VOC consumption at urban center (MEM and YH, 4-6ppbv) was lower than that in outer areas (JK and GS, 9-11ppbv), and the average increment of O_3 at 14:00 LT was higher than that at 07:00 LT in marginal area, suggesting more efficient photochemical reactions at JK and GS. Meanwhile, the average values of $[\bullet OH]\triangle t$ for each site, ranked in the same order with VOCs consumption, were varied in a range of 2.9×10^{10} to $4.7\times10^{10}cm^{-3}$ s. The values were slightly lower than the results of $4.9\times10^{10}cm^{-3}$ s measured at Beijing in August-September, 2010 (Yuan et al., 2012), indicating that comparatively less aging process in Zhengzhou.

Taken the decrement of VOCs and NO_x as independent variable and the increment of O_3 as dependent variable, the multiple regression analysis was performed. The results for JK and GS were presented as:

$[O_3]_{increment}=0.41[VOC]_{decrement}+0.20[NO_x]_{decrement}+53.4$ (JK, $R^2=0.44$)

$[O_3]_{increment}=0.34[VOC]_{decrement}+0.39[NO_x]_{decrement}+59.3$ (GS, $R^2=0.38$)

The F values for JK and GS were 16.1 and 10.1 respectively, indicating the regression results at the two sites were acceptable. However, the relationships among O_3, NO_x and VOCs could not be expressed in this way at MEM and YH, where the low values for both R^2 (0.12, 0.09) and F values (2.7, 2.8). This potentially attributed to more constant disturbance from fresh emission sources at urban center.

4. Conclusions

In this study, VOC samples were collected at four sites in Zhengzhou, Henan (China) for the first time and analyzed for 57 species. It is found that the weighted percentage of aromatics was lower, while alkyne was higher in Zhengzhou city than in other Chinese cities. C2 - C5 alkanes, acetylene, ethylene, toluene and benzene were the most abundant VOCs in the region, suggesting widespread combustion-related sources in the city. Median concentrations for the four sites are almost indistinguishable but, based on monthly averages, the maximum Σ_{VOCs} was observed at GS

site, because it is occasionally impacted by emissions from the nearby gas fueled plant, which strongly skew the distribution of measured VOC concentrations. Approximately 75% of VOCs/NO$_x$ ratios were below 6 at each site, indicating that the O$_3$ formation was driven by VOCs regionally. Different from other megacities, alkenes were the biggest contributors to OFP, and acetylene was particularly critical at each site. In addition, the impact of aging process was less in Zhengzhou than that Beijing. Photochemical processing appears to be more efficient at JK and GS, while the relationships among O$_3$, NO$_x$ and VOCs at urban sites of MEM and YH were more complex.

Our analysis of ozone formation does not take into account the important effects of transport and mixing, and should be viewed in this light. Both measured mixing ratios and calculated OFPs demonstrated that the most important contributors to VOCs were vehicle exhaust, coal+biomass burning and solvent use, illustrating the necessary to conduct emission controls on these pollution sources. Vehicle emission was more dominant at urban center (YH and MEM), while solvent use was more important at the sites (JK and GS) far away from urban center in Zhengzhou. It is further shown that the air pollution in Zhengzhou was usually impacted by local emissions, with no more than 50% of 48-hour backward trajectories extended out of Henan province in June, August and September, and southern air clusters occasionally from Hubei Province was cleaner. In addition, strong emissions for coal+biomass burning were concentrated in southwest of Shanxi, western of Shandong and southwest of Henan provinces according to the PSCF analysis. Due to less anthropogenic emissions and more favorable dispersion conditions, most of the air pollutants had the lowest levels in the mid-summer month of July. This study provides the first-hand information on the characteristics of VOCs and assists in overcoming the O$_3$ pollution issue in Zhengzhou city, China.

Acknowledgements

The authors would like to thank for valuable suggestions, corrections, and discussions from both anonymous referees and editor, Prof. Rob MacKenzie. Their comments are particularly important and greatly contributed to improve this work. This research was supported by the Key Program of National Natural Science Foundation of China (Grant No. 91744209).

Table & Figure

Table1. Mean concentrations of Σ_{VOCs} (ppbv) and correspondent standard deviations (SD) at every site during the

sampling period

	JK		MEM		GS		YH	
	Mean	SD	Mean	SD	Mean	SD	Mean	SD
May.2017	37.6	22.6	29.3	15.3	31.7	18.7	30.1	16.4
June.2017	34.0	19.9	30.3	12.8	39.3	25.4	28.3	11.9
July.2017	16.0	6.1	20.7	12.7	19.6	13.9	15.9	7.5
Aug.2017	21.5	15.3	24.4	20.8	20.5	15.7	26.1	17.0
Sept.2017	26.2	16.2	34.2	23.8	30.4	19.8	32.6	19.8

Table2. Wind speed (m s^{-1}) measured about 10m above ground level at every site during the sampling period

	JK	MEM	YH	GS
May	1.34±0.65	1.86±1.19	1.27±0.66	0.97±0.49
June	1.07±0.48	1.86±0.94	0.97±0.36	0.74±0.33
July	1.48±0.59	2.62±1.19	1.15±0.45	0.90±0.32
August	1.06±0.48	1.86±0.94	0.95±0.39	0.76±0.35
September	0.80±0.38	1.24±0.80	0.82±0.43	0.62±0.38

557 Table3. Concentration levels of VOCs and compositions of major groups in Zhengzhou and other cities in China

Items		Guangzhou	Nanjing	Beijing	Hangzhou	Wuhan	Zhengzhou
		March-December, 2005	2011-2012	August, 2006	July-August, 2013	2013-2014	May-September, 2017
Sampling site		residents-commercial-transportation mixed area	transportation-industry mixed area	residents-commercial mixed area	residents-transportation mixed area	urban	urban
Quantified compounds		59 NMHC	56 NMHC	47 NMHC	56 NMHC	99 VOCs	56 NMHC
Total samples		145	_	24	_	_	400
TNMHC (ppbv)		47.3	43.5	65.6±17.4	55.9	23.3±0.5	29.2±23.1
Compositions of major groups (%)	alkane	49.0	45.0	52.3	33.2		56.7±12.4
	alkene	16	25.3	21.2	25.9		16.2±7.6
	aromatic	23	22.3	18.1	24.3		14.1±8.4
	alkyne	12	7.3	8.4	16.6		12.9±6.7
Reference		(Li and Wang, 2012)	(An et al., 2014)	(Guo et al., 2012)	(Li et al., 2017b)	(Lyu et al., 2016)	this study

558

559

560

561

562

563

Table4. Specific information on VOCs, O_3 and NO at the four sites in June, 2017

Composition or conc.	JK	MEM	YH	GS
Aromatic (%)	9.06	11.6	4.72	15.8
Alkene (%)	6.36	4.13	5.52	5.47
Σ_{VOCs} (ppbv)	34.0	30.3	28.3	39.3
O_3(ppbv)	74.9	73.5	73.8	88.0
NO(ppbv)	7.10	7.72	2.34	4.47

564

565

566

567

568

569

570

571

572

573

574

575

576

577

578

579

580

581

582   Table5. Top 10 VOCs ranked according to calculated ozone formation potential (OFP) and their corresponding

583   percentage weighted in mixing ratio

Site	Species	OFP (ppbv)	Weighted in OFP (%)	Weighted in mixing ratio (%)	Site	Species	OFP (ppbv)	Weighted in OFP (%)	Weighted in mixing ratio (%)
	Ethylene	19.0	25.5	8.22		Ethylene	18.4	30.9	7.92
	Isoprene	13.0	21.8	7.31		Isoprene	4.66	10.1	2.36
	m/p-Xylene	6.08	5.89	2.67		Toluene	3.73	6.67	3.99
	Toluene	5.53	5.83	4.22		Propylene	3.60	6.16	1.25
	Propylene	4.03	5.36	1.29		Acetylene	2.82	5.00	12.2
JK	Acetylene	2.97	4.44	13.5	MEM	m/p-Xylene	2.55	4.20	1.40
	n-Butane	2.15	3.05	7.28		n-Butane	1.81	3.20	5.97
	o-Xylene	1.83	2.00	0.88		Isopentane	1.76	3.16	7.39
	Isopentane	1.66	1.95	6.50		Ethane	1.58	2.96	23.4
	Propane	1.17	1.73	9.77		Propane	1.31	2.48	10.6
	Ethylene	19.8	28.1	8.88		Ethylene	18.1	26.90	7.51
	Isoprene	7.44	11.3	3.67		Isoprene	8.01	16.8	4.64
	Toluene	6.63	7.75	5.72		Toluene	7.43	7.67	5.49
	m/p-Xylene	3.93	4.38	1.58		Propylene	4.39	5.85	1.26
	Acetylene	3.15	4.38	13.9		m/p-Xylene	4.31	4.57	1.75
YH	Propylene	3.01	3.60	0.91	GS	Acetylene	2.76	4.24	12.1
	Trans-2-pentene	2.25	2.94	3.43		n-Butane	1.82	2.93	6.39
	n-Butane	1.84	2.80	6.31		Isopentane	1.71	2.68	6.94
	Isopentane	1.59	2.22	6.69		Propane	1.38	2.26	11.6
	Propane	1.18	1.98	10.2		Isobutane	1.13	1.98	4.59

584   [a] m-Xylene and p-Xylene are co-eluted in the chromatographic separation.

585

586

587
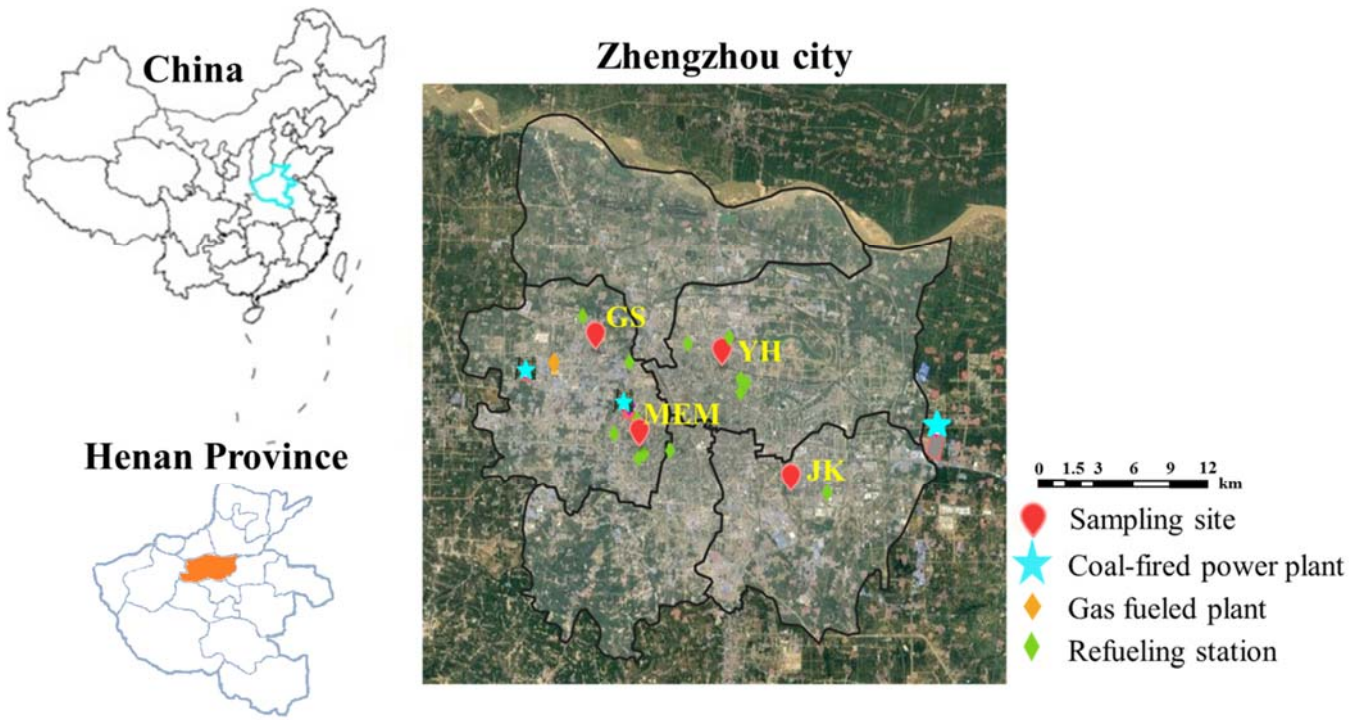
Fig 1. Satellite imagery showing the four sampling sites and surrounding areas of Zhengzhou, China, including

major emission sources presented with different marks

590
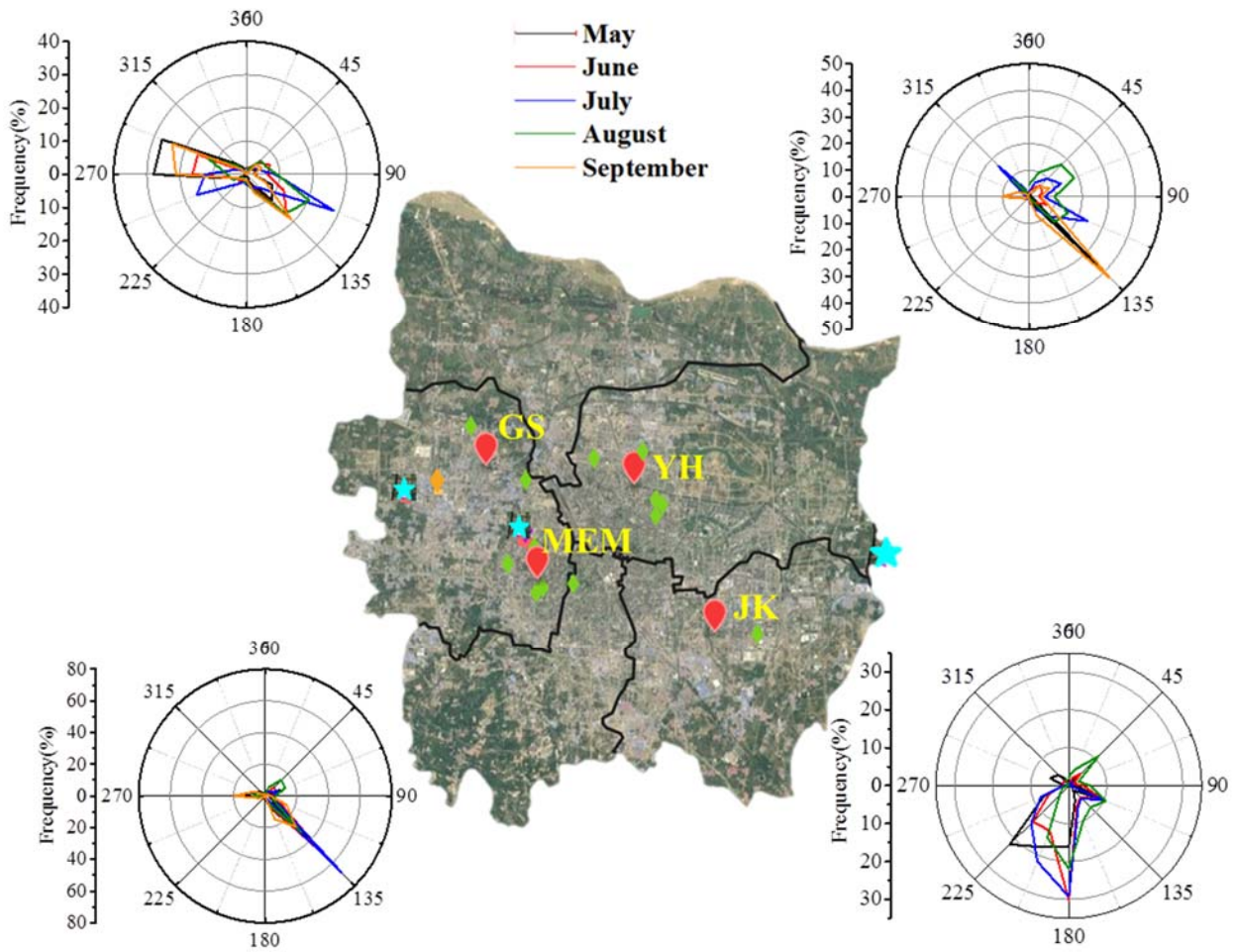
591

592   Fig.2 Wind direction for each site during May to September, 2017

593

May   June

July   August

September
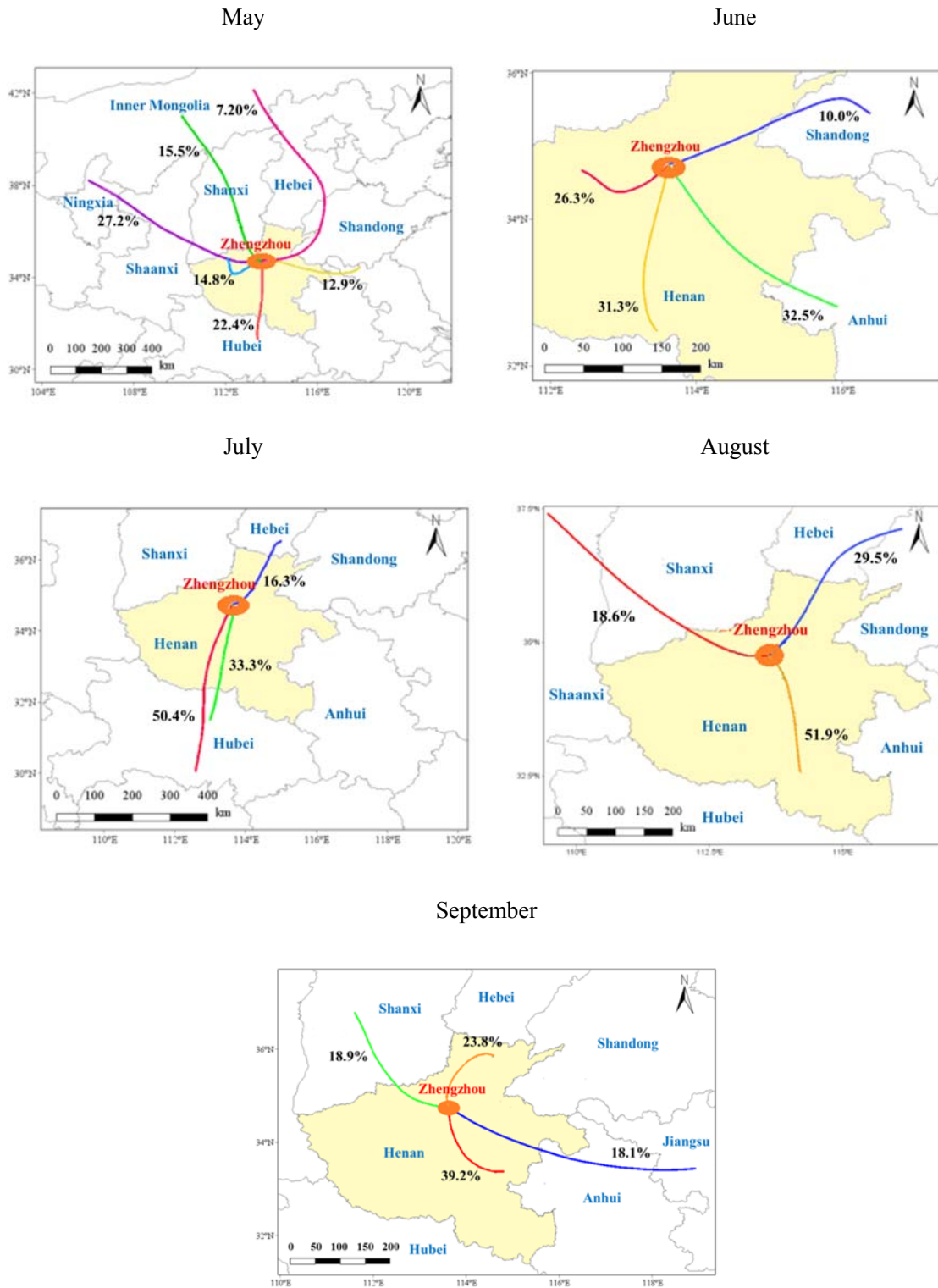
Fig. 3 Cluster analysis of 48-hour backward trajectories for Zhengzhou in each sampling month, with the start height at 500m altitude and running interval set as 2- hour for each day, percentage of each cluster and covered areas are presented as well.
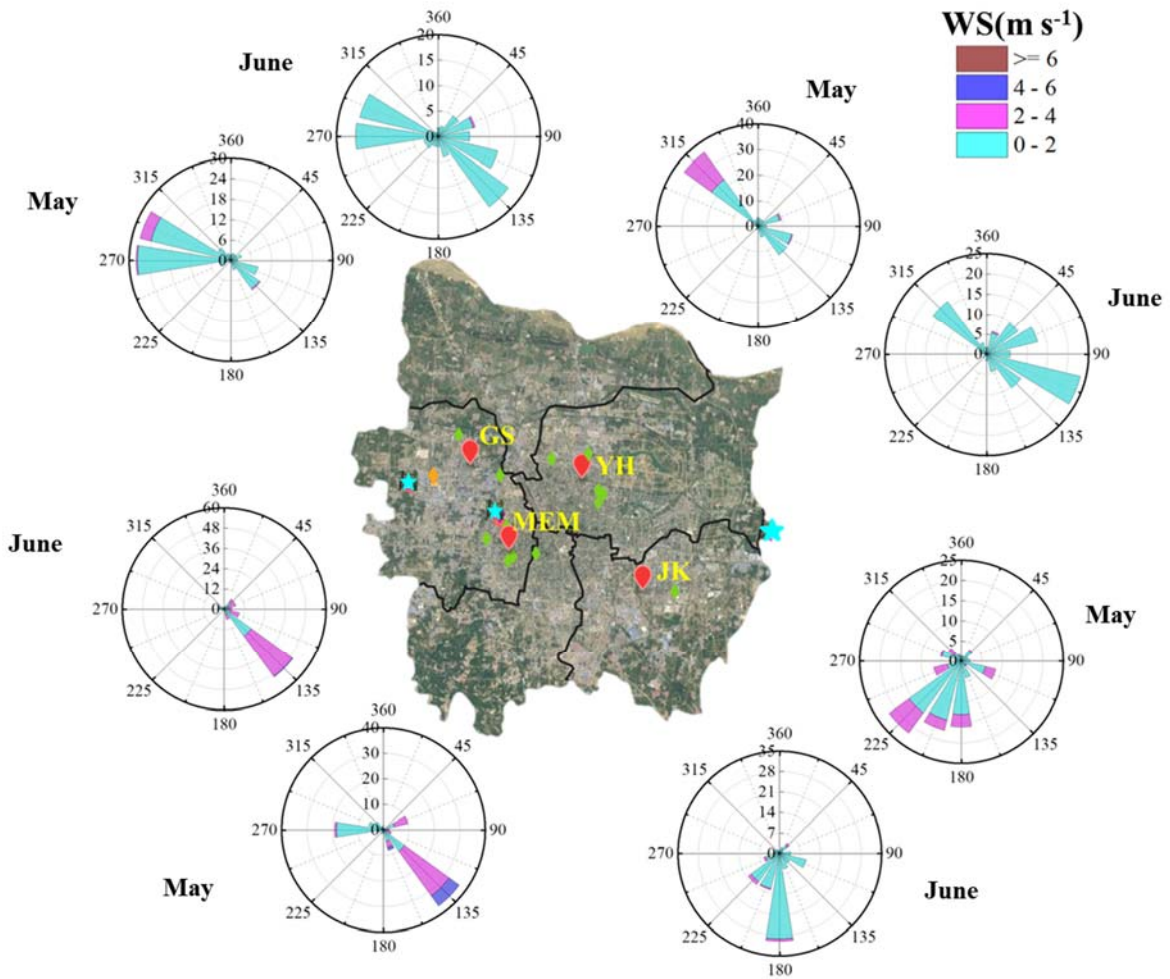
597

598   Fig.4 Wind rose plot showing wind sector frequency (%) of occurrence and associated wind speed (m s⁻¹) at each

599   site in May and June (the wind distribution in other three months were illustrated in Fig S2), which were recorded

600   by the anemometers placed at the same site with other air monitors.

601

602

603
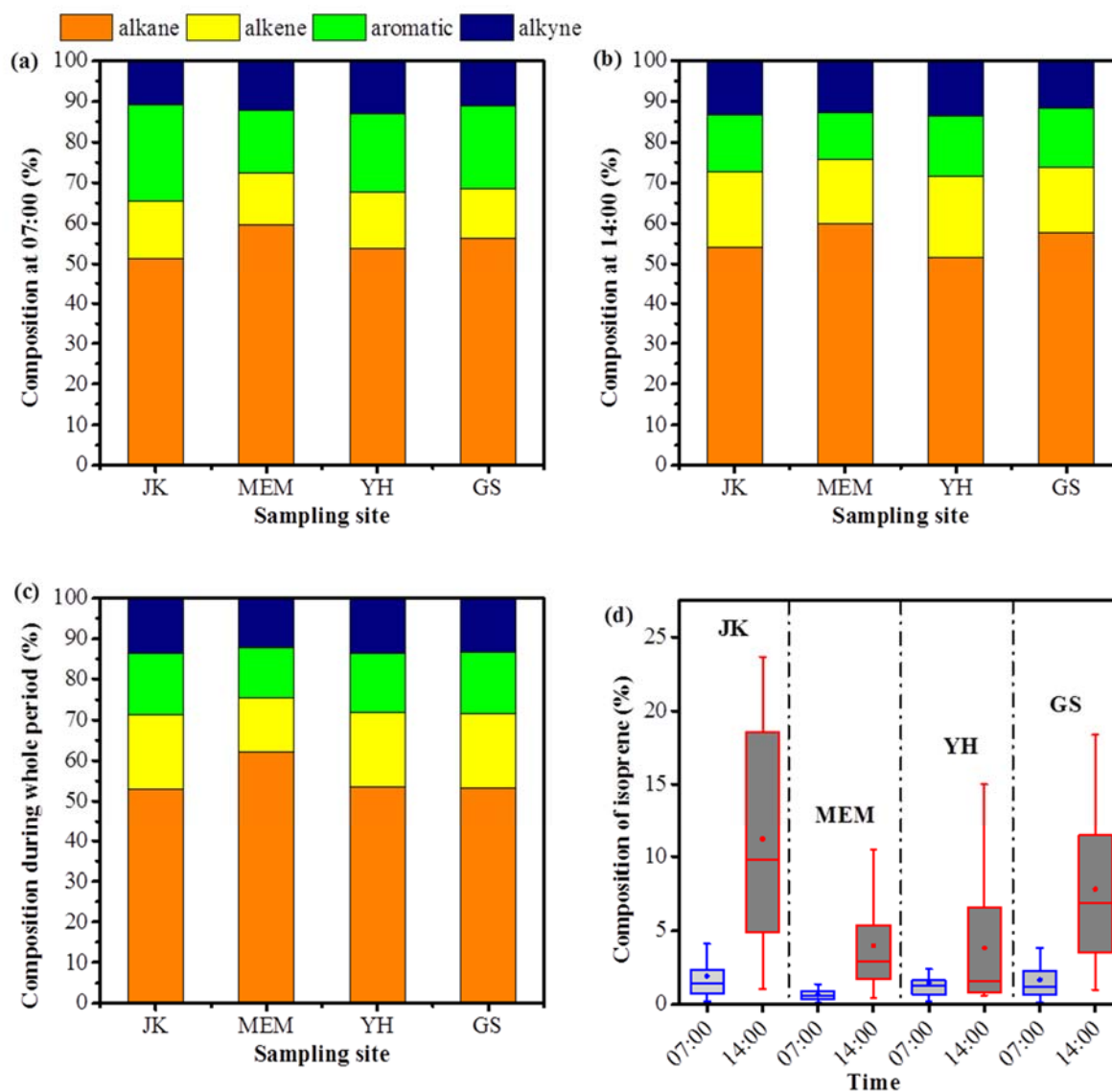
Fig. 5 Compositions of major organic classes at 07:00 LT (a), 14:00 LT (b) and during the whole sampling period

(c) at the four sites, and the box plot for the composition of isoprene at 07:00 LT and 14:00 LT for each site, with

the whiskers range in 5-95%iles, and the box shows the 25-75%iles, the solid dots represents the arithmetic

average, the line in the box shows the median (d).

608

609

610
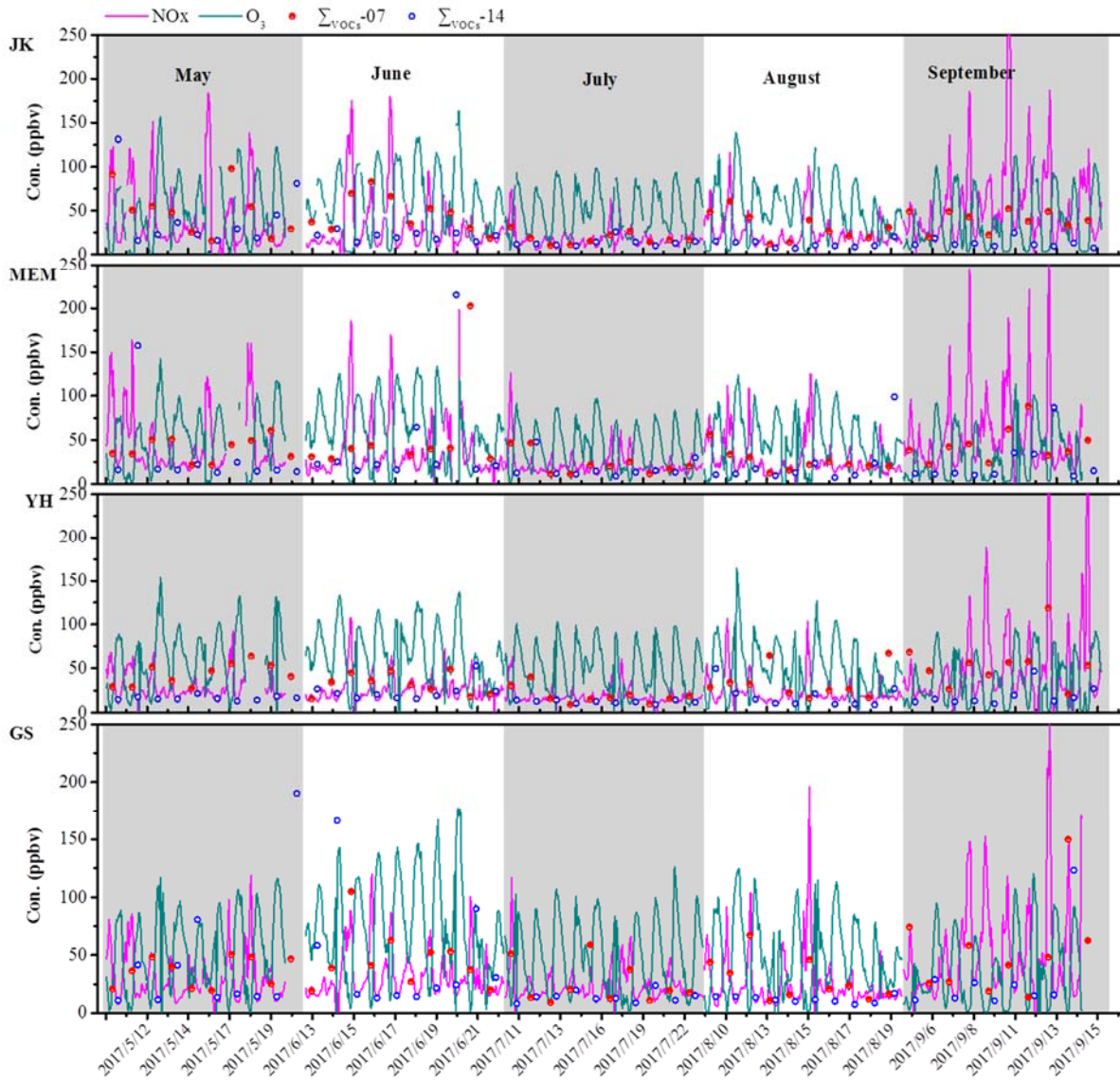
Fig.6 Temporal variations of mixing ratios of Σ_{VOCs}, NO_x and O_3 at the four sites during the whole sampling period, in which Σ_{VOCs}-07 stands for the concentration level of Σ_{VOCs} observed at 07:00 LT, and Σ_{VOCs}-14 was that observed at 14:00 LT.

614

615

616
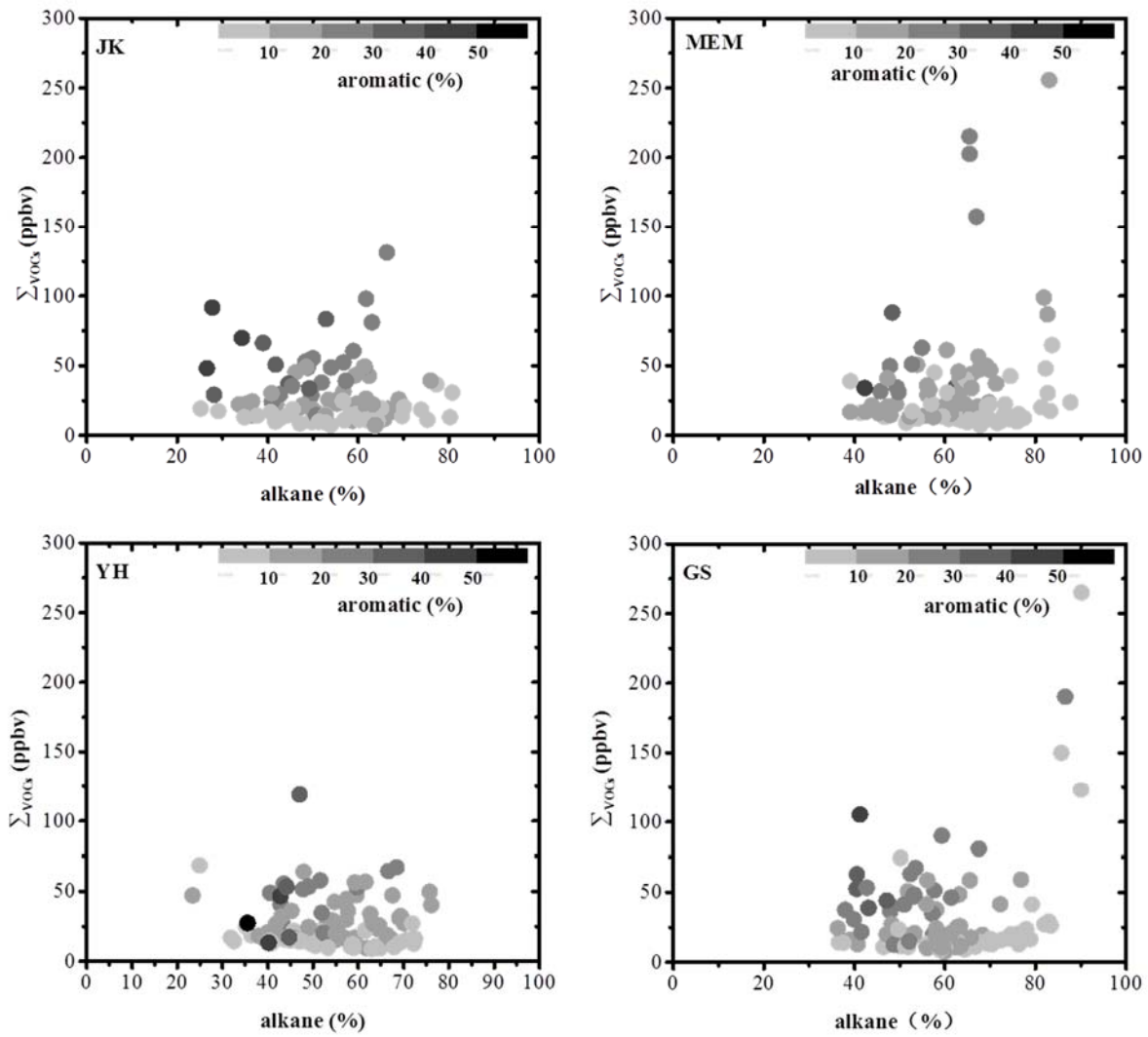
Fig. 7 The relationship between mixing ratio of Σ_{VOCs} and the composition of alkane, the data points are color coded with the composition of aromatic.

617

618

619

620

621
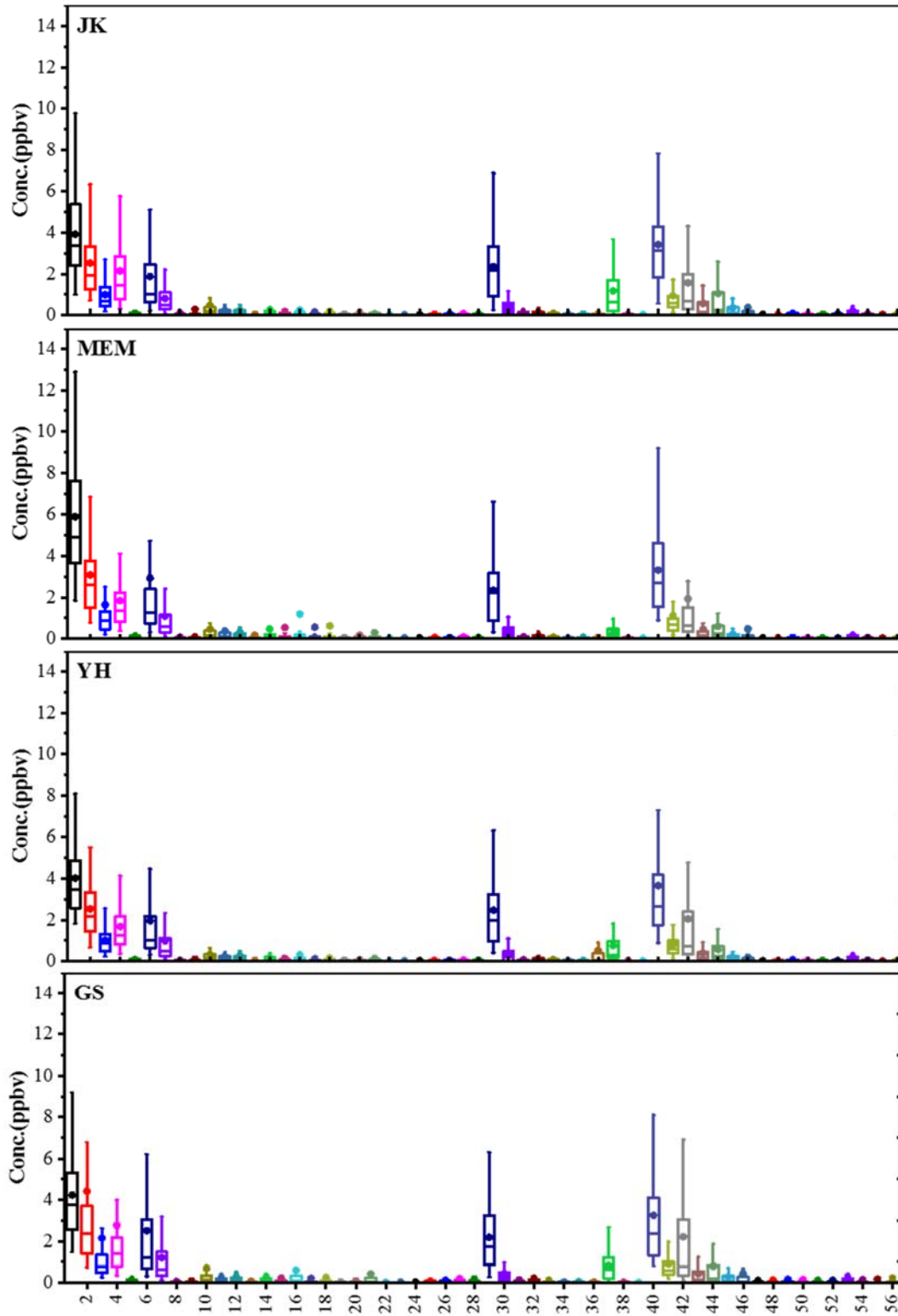
Fig.8 Concentrations of 57 VOCs at each site for the whole sampling period, the whiskers show the 5-95%iles,

and the box shows the 25-75%iles, the solid points shows the arithmetic average, the line in the box shows the

median. The chemicals are listed in Table S1.

625
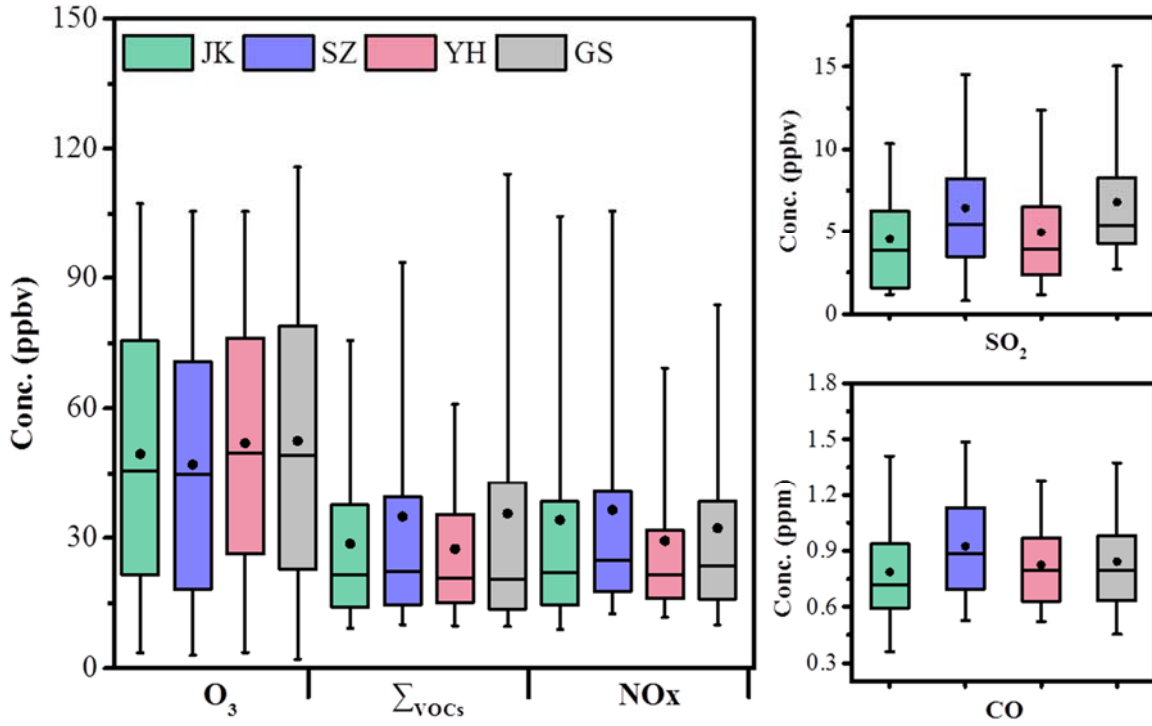
626 Fig. 9 The distribution of concentration point on O_3, Σ_{VOCs}, NO_x, SO_2 and CO at each site, the range of the box

627 was 25%-75%, the black line in the box stands for median level, the black dot represent the average level, the

628 range of whisker was 5-95%.

629

630
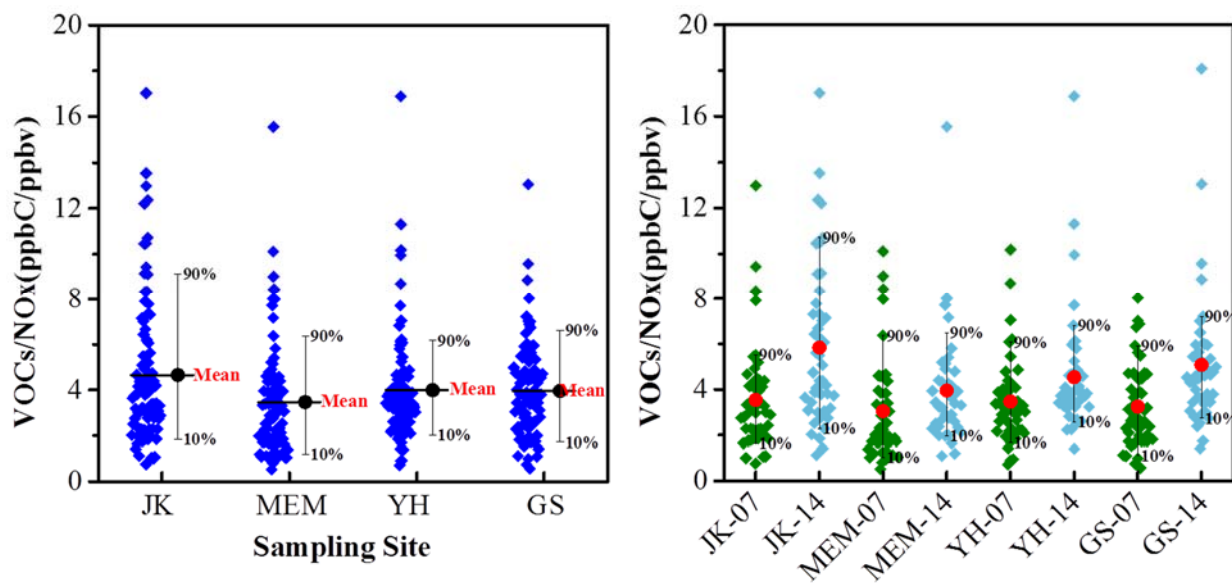
Fig.10 The data distribution of VOCs/NO$_x$(ppbC/ppbv) at the four sites (left), and the ratio observed at 07:00 LT

and 14:00 LT were presented (right).

633

634
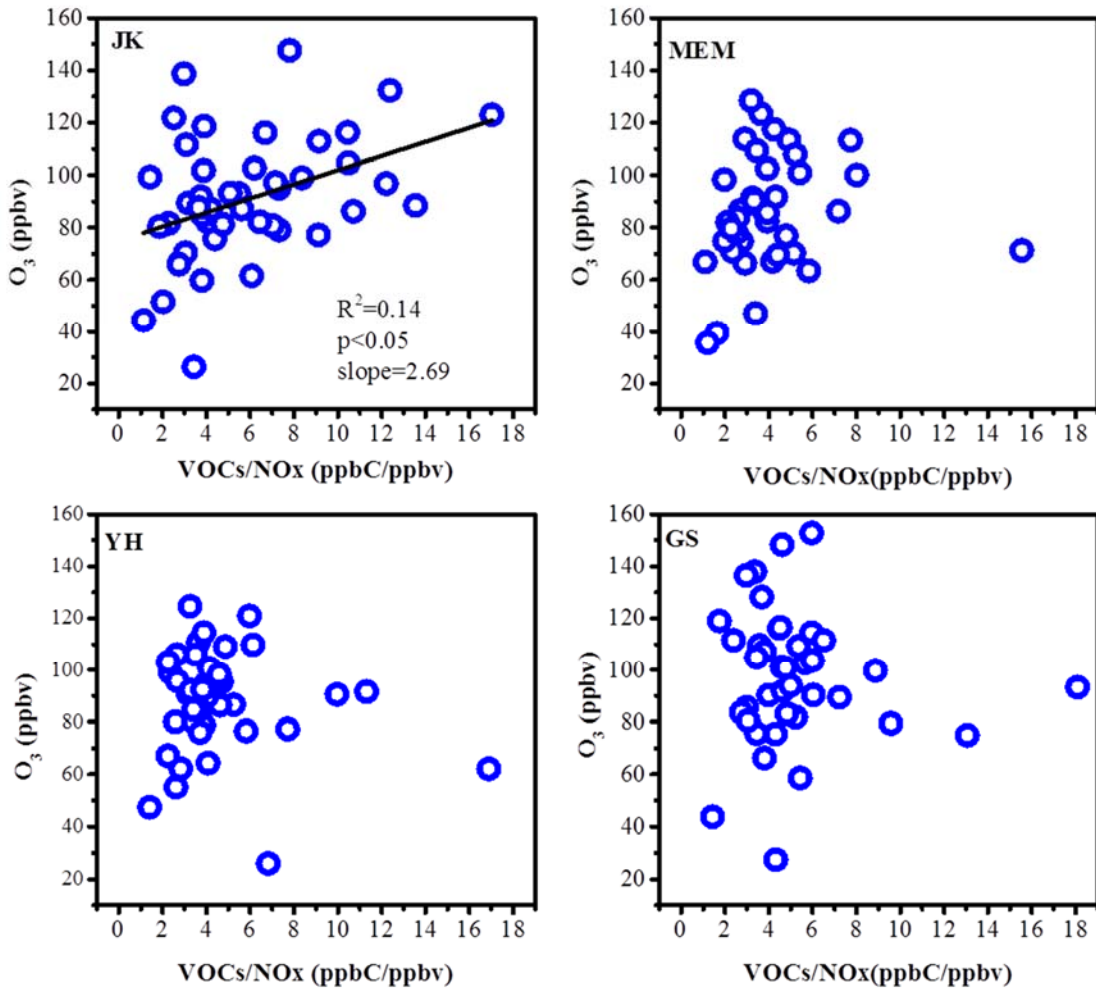
635   Fig.11 The relationship between O_3 and VOCs/NO_x at 14:00 LT for each of the four sampling sites.

636

637

638
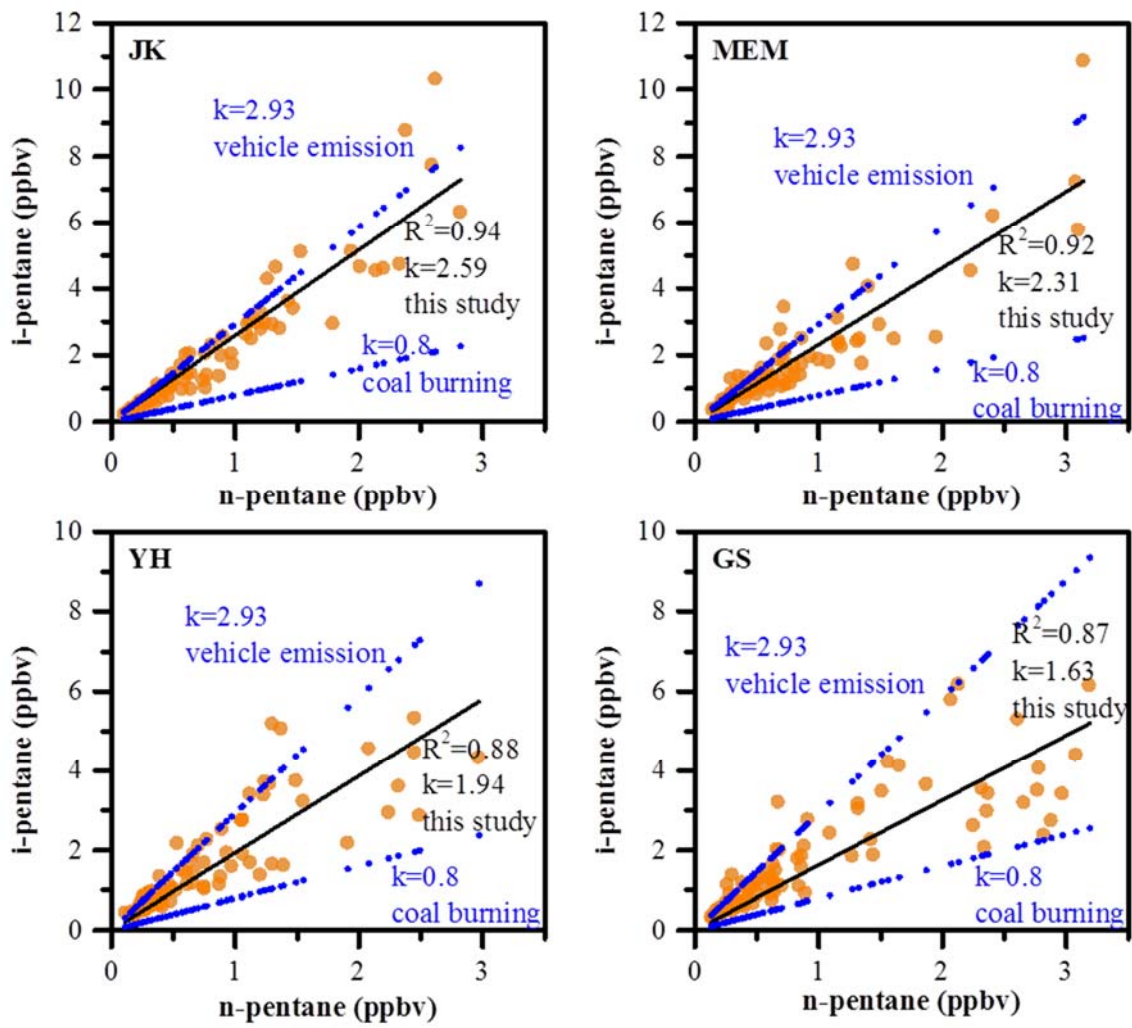
Fig. 12 Ratios of isopentane to n-pentane at every site

643
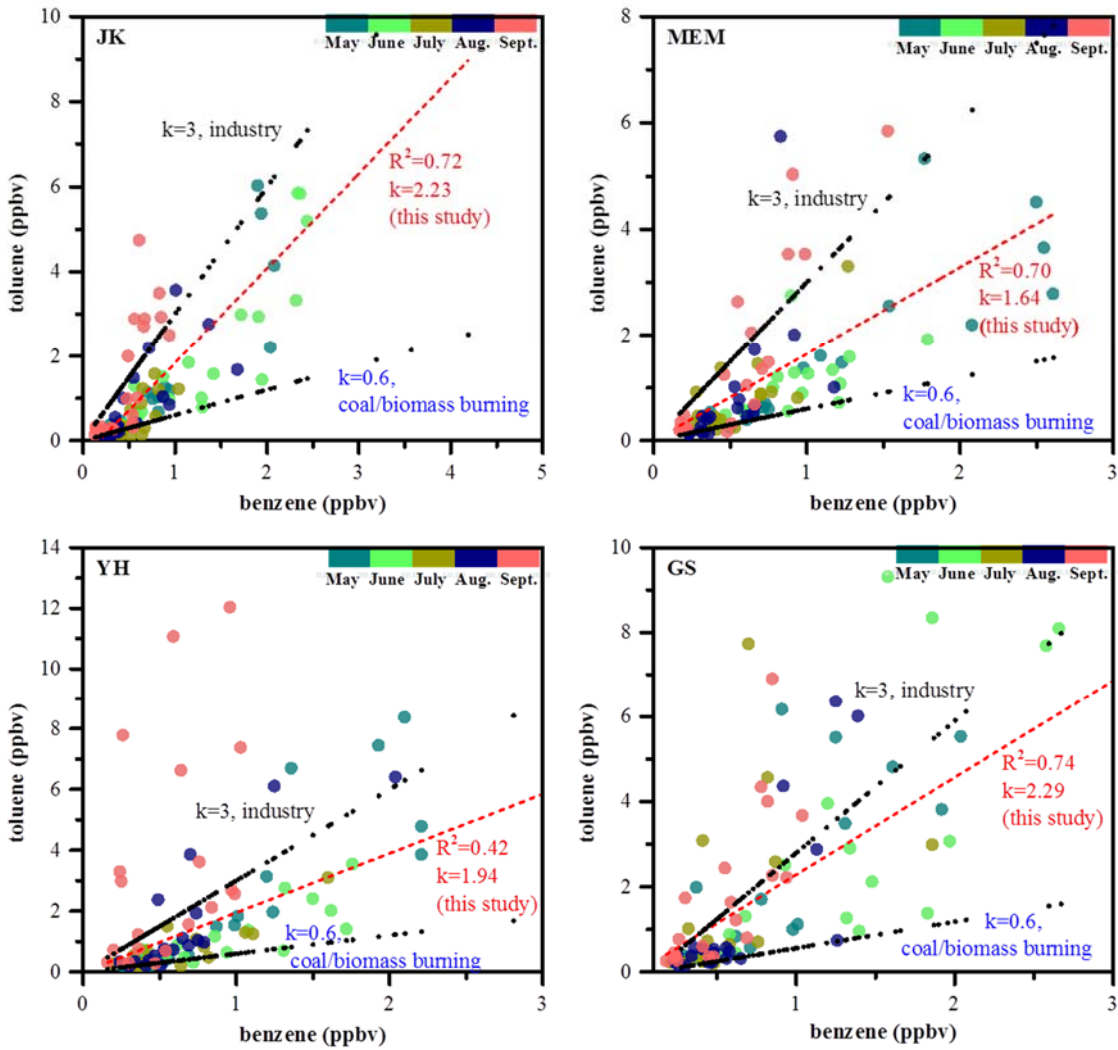
Fig.13 T/B ratios and linear correlation coefficients (R^2) between benzene and toluene at every site, the data points were color mapped with sampling period.

644

645

646

647

648
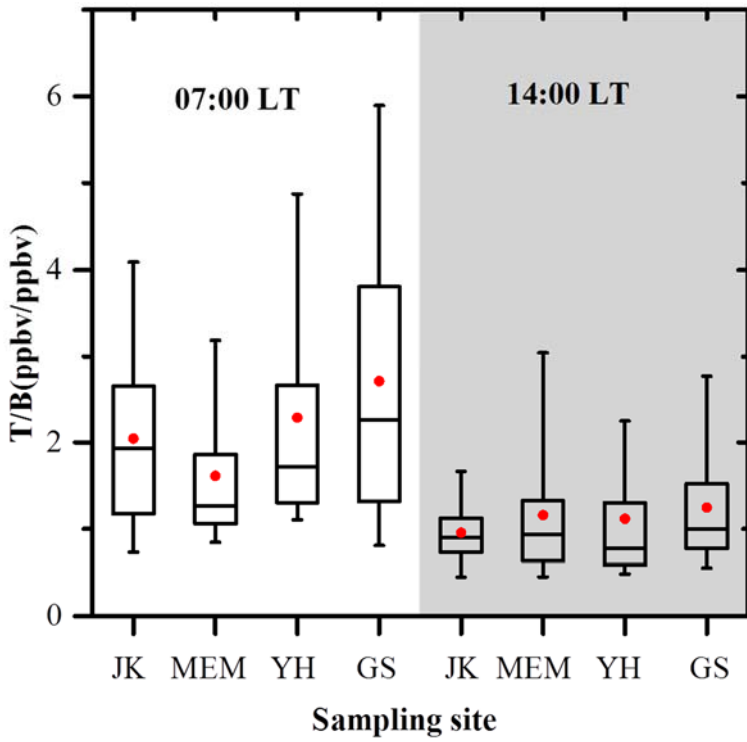
649

650   Fig. 14 The average ratio of T/B at 07:00LT and 14:00LT for each site during the whole sampling period

651

652
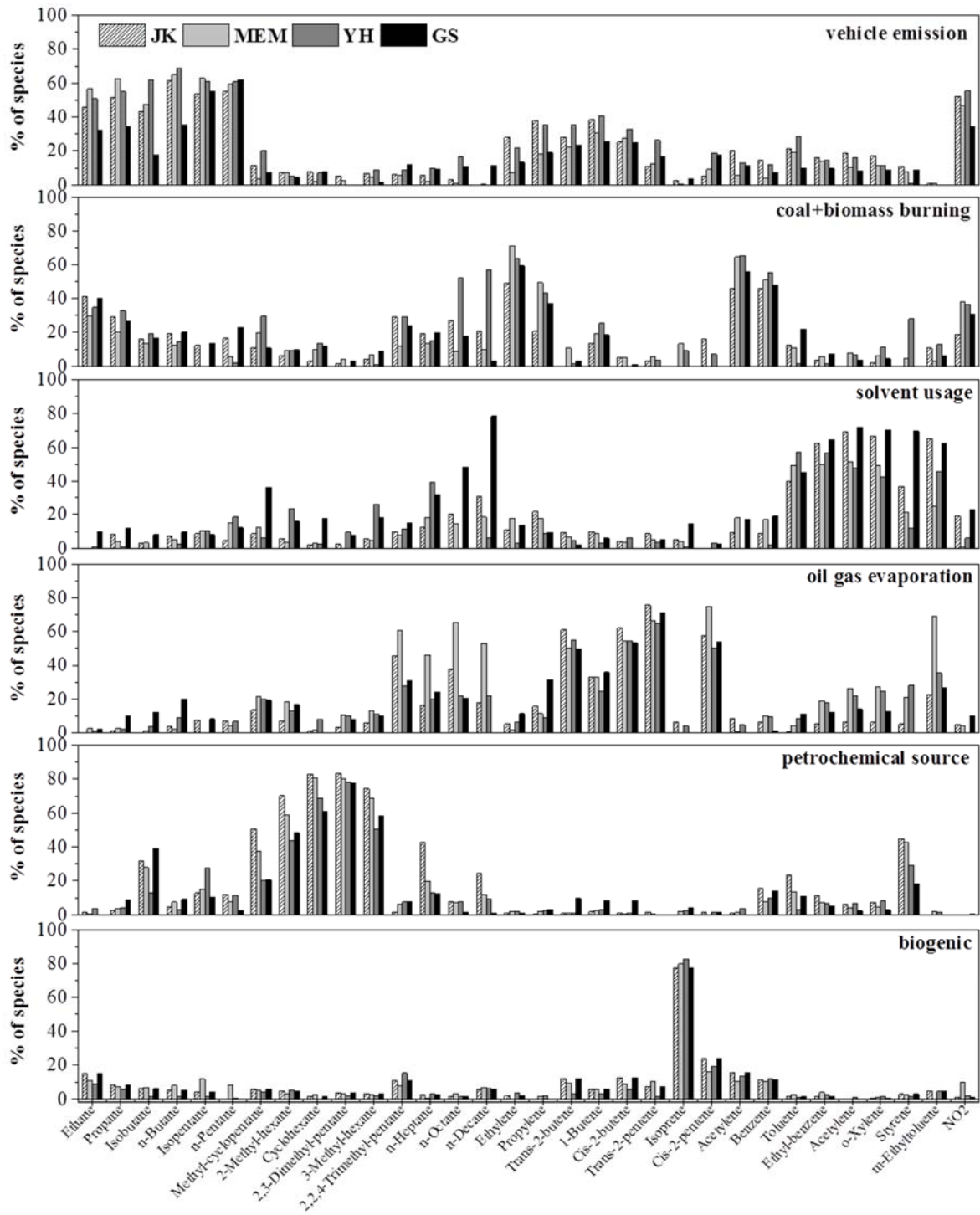
Fig. 15 Factor profiles of major emission sources, namely vehicle emission, coal+biomass burning, solvent

usage, oil gas evaporation, petrochemical and biogenic source resolved by PMF model.

653

654

655

656

657
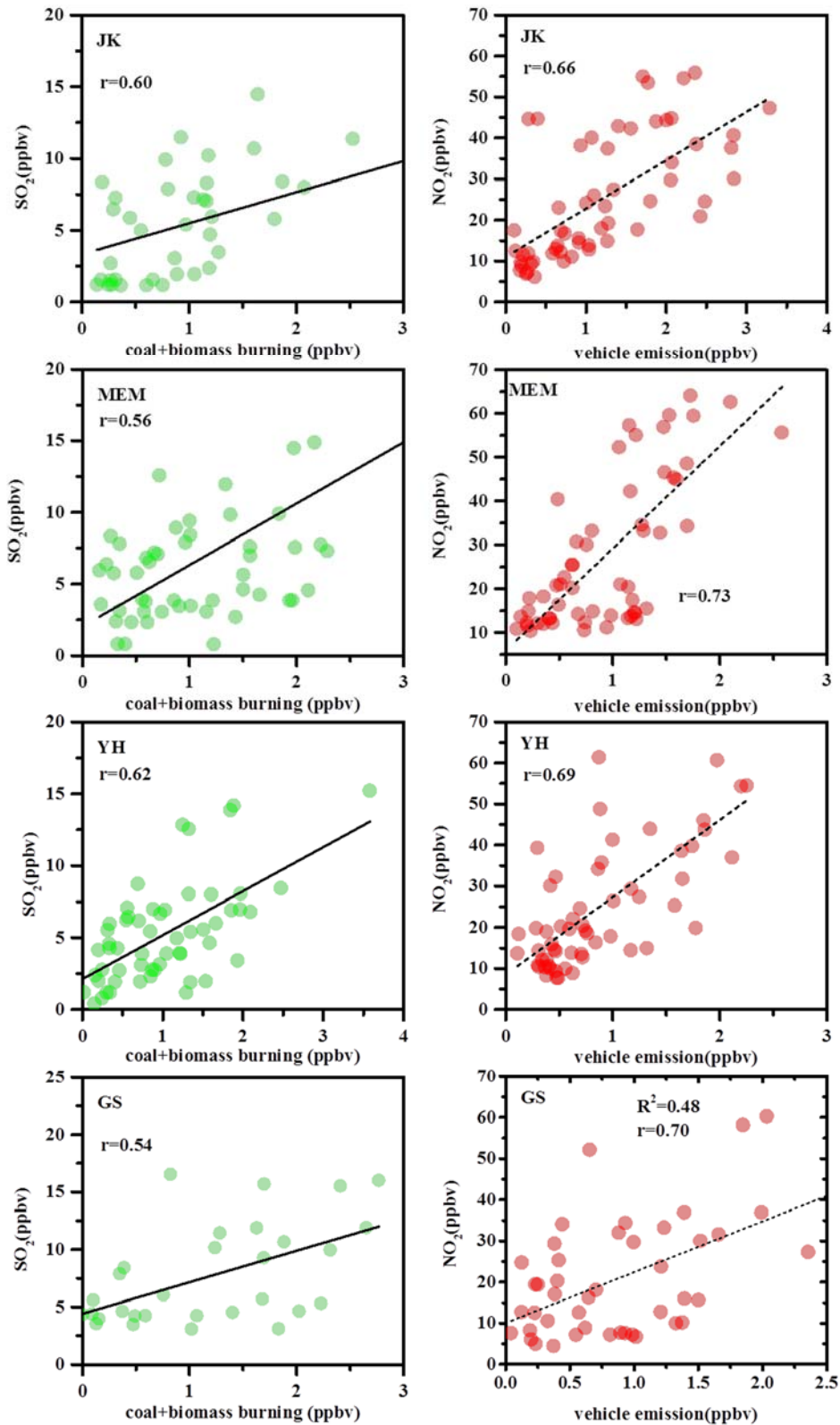
Fig. 16 Correlation analysis relating source-apportioned VOC contributions of coal+biomass burning (left column) and vehicle emission (right column) with co-located measurements of SO_2 and NO_2 for each site (rows).

660
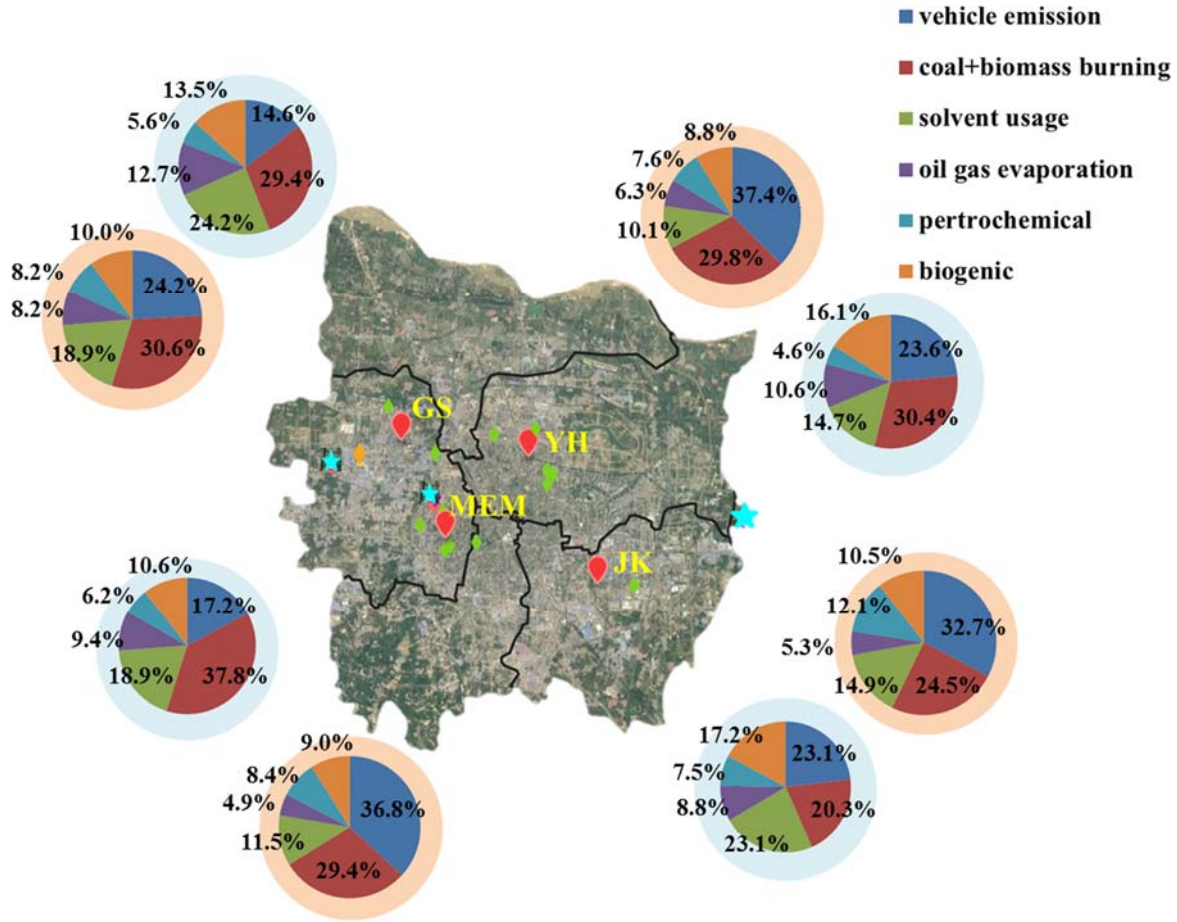
661

662   Fig. 17 Source apportionment results during the whole sampling period. The results weighted in observed

663   concentrations were shadowed with pink color, and the results estimated based on OFP were shadowed with light

664   blue color.

665

666

667

668

669
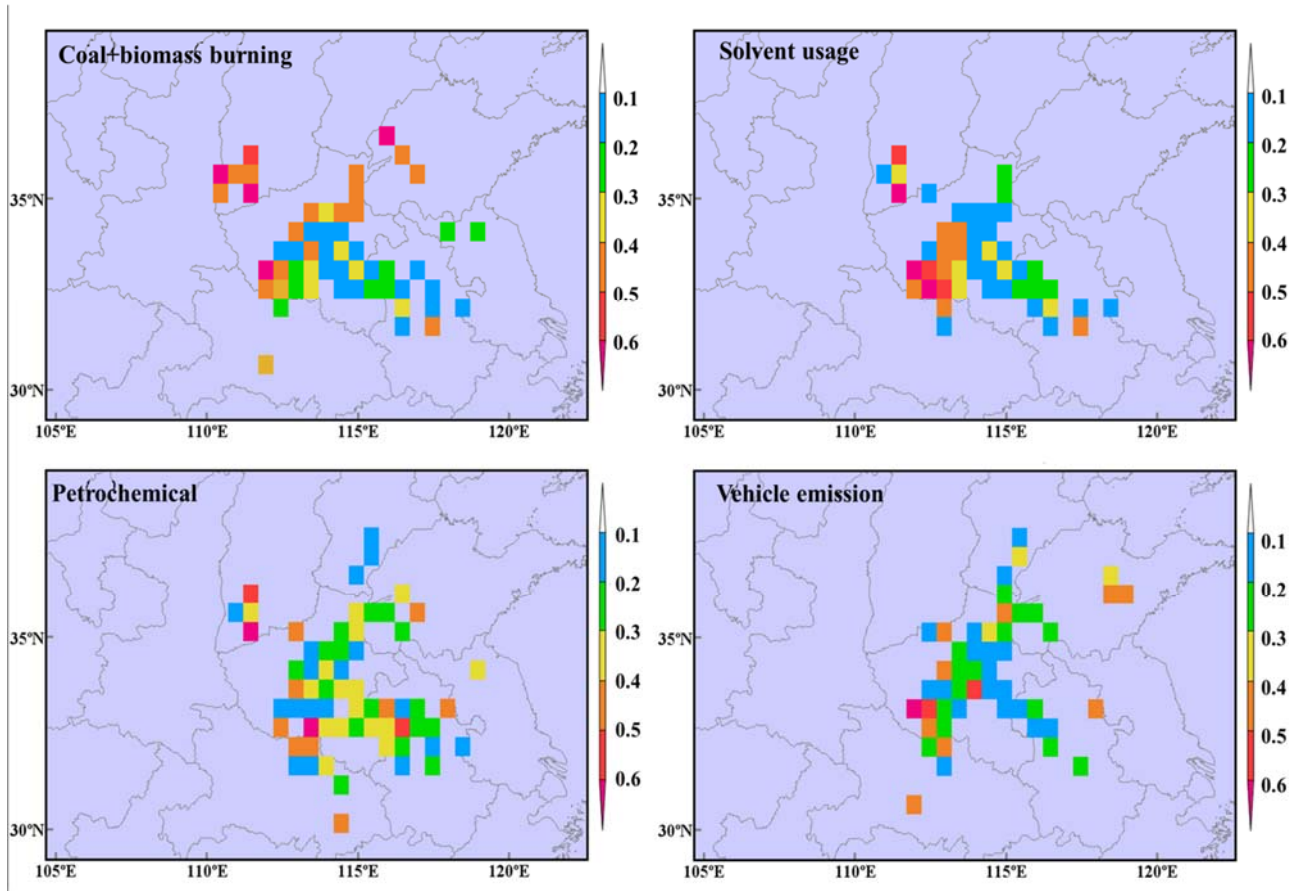
Fig. 18 Probable source regions apportioned by PSCF at Zhengzhou at summer (June-Aug. 2017) during

sampling period

670

671

672

673

674

675 **Reference**

676 Abeleira, A., Pollack, I. B., Sive, B., Zhou, Y., Fischer, E. V., and Farmer, D. K.: Source

677 characterization of volatile organic compounds in the Colorado Northern Front Range Metropolitan

678 Area during spring and summer 2015, J. Geophys. Res.-Atmos., 10.1002/2016jd026227, 2017.

679 Akagi, S. K., Yokelson, R. J., Wiedinmyer, C., Alvarado, M. J., Reid, J. S., Karl, T., Crounse, J. D.,

680 and Wennberg, P. O.: Emission factors for open and domestic biomass burning for use in

681 atmospheric models, Atmos. Chem. Phys., 11, 4039-4072, 10.5194/acp-11-4039-2011, 2011.

682 An, J., Zhu, B., Wang, H., Li, Y., Lin, X., and Yang, H.: Characteristics and source apportionment

683 of VOCs measured in an industrial area of Nanjing, Yangtze River Delta, China, Atmos. Environ.,

684 97, 206-214, 10.1016/j.atmosenv.2014.08.021, 2014.

685 Barletta, B., Meinardi, S., Sherwood Rowland, F., Chan, C.-Y., Wang, X., Zou, S., Yin Chan, L.,

686 and Blake, D. R.: Volatile organic compounds in 43 Chinese cities, Atmos. Environ., 39,

687 5979-5990, 10.1016/j.atmosenv.2005.06.029, 2005.

688 Borbon, A., Locoge, N., Veillerot, M., Galloo, J. C., and Guillermo, R.: Characterisation of

689 NMHCs in a French urban atmosphere: overview of the main sources, Sci. Total Environ., 292

690 177–191, 2002.

691 Carter, W. P. L.: Development of Ozone Reactivity Scales for Volatile Organic Compounds, J. Air

692 & Waste Manage. Assoc., 44, 881-899, 1994.

693 Carter, W. P. L.: Development of the SAPRC-07 Chemical Mechanism and Updated Ozone

694 Reactivity Scales, available at: http://www.cert.ucr.edu/~carter/SAPRC, (last accesse: 13 March,

695 2018), 2010.

696 Chen, W. T., Shao, M., Lu, S. H., Wang, M., Zeng, L. M., Yuan, B., and Liu, Y.: Understanding

697 primary and secondary sources of ambient carbonyl compounds in Beijing using the PMF model,

698 Atmos. Chem. Phys., 14, 3047-3062, 10.5194/acp-14-3047-2014, 2014.

699 Cheng, L., Fu, L., Angle, R. P., and Sandhu, H. S.: Seasonal variations of volatile organic

700 compounds in Edmonton, Alberta, Atmos. Environ., 31, 239-246, 1997.

701 Choek, D. P., and Heuss, J. M.: Urban ozone and its precursors, Environ. Sci. Technol., 21,

702 1146-1153, 1987.

703 Chinese Ministry of Environmental Protection: Ambient Air Quality Index (AQI) Technical

704 Provisions (Trial), available at:

705 http://kjs.mee.gov.cn/hjbhbz/bzwb/jcffbz/201203/t20120302_224166.shtml, (last access: 03

706 November, 2018), 2012.

707 Duan, J., Tan, J., Yang, L., Wu, S., and Hao, J.: Concentration, sources and ozone formation

708 potential of volatile organic compounds (VOCs) during ozone episode in Beijing, Atmos. Res., 88,

709 25-35, 10.1016/j.atmosres.2007.09.004, 2008.

710 Fujita, E. M., Watson, J. G., Chow, J. C., and Lu, Z.: Validation of the chemical mass balance

711 receptor model applied to hydrocarbon source apportionment in the southern California air quality

712 study, Environ. Sci. Technol., 28, 1633-1649, 1994.

713 Fujita, E. M.: Hydrocarbon source apportionment for the 1996 Paso del Norte Ozone Study, Sci.

714 Total Environ., 276, 171-184, 2001.

715 Gao, W., Tie, X., Xu, J., Huang, R., Mao, X., Zhou, G., and Chang, L.: Long-term trend of O_3 in a

716 mega City (Shanghai), China: Characteristics, causes, and interactions with precursors, Sci. Total

717 Environ., 603-604, 425-433, 10.1016/j.scitotenv.2017.06.099, 2017.

718 Geng, N., Wang, J., Xu, Y., Zhang, W., Chen, C., and Zhang, R.: PM2.5 in an industrial district of

719 Zhengzhou, China: Chemical composition and source apportionment, Particuology, 11, 99-109,

720 10.1016/j.partic.2012.08.004, 2013.

721 Gentner, D. R., Worton, D. R., Isaacman, G., Davis, L. C., Dallmann, T. R., Wood, E. C., Herndon,

722 S. C., Goldstein, A. H., and Harley, R. A.: Chemical composition of gas-phase organic carbon

723 emissions from motor vehicles and implications for ozone production, Environ. Sci. Technol., 47,

724 11837-11848, 10.1021/es401470e, 2013.

725 Gilman, J. B., Lerner, B. M., Kuster, W. C., and de Gouw, J. A.: Source signature of volatile

726 organic compounds from oil and natural gas operations in northeastern Colorado, Environ. Sci.

727 Technol., 47, 1297-1305, 10.1021/es304119a, 2013.

728 Gong, M., Yin, S., Gu, X., Xu, Y., Jiang, N., and Zhang, R.: Refined 2013-based vehicle emission

729 inventory and its spatial and temporal characteristics in Zhengzhou, China, Sci. Total Environ.,

730 599-600, 1149-1159, 10.1016/j.scitotenv.2017.03.299, 2017.

731 Guenther, A., Hewitt, C. N., Erickson, D., Fall, R., Geron, C., Graedel, T., Harley, P., Klinger, L.,

732 Lerdau, M., McKay, W. A., Pierce, T., Scholes, B., Steinbrecher, R., Tallamraju, R., Taylor, J., and

733 Zimmerman, P.: A global model of natural volatile organic compound emissions, J. Geophys. Res.,

734 100, 8873-8892, 1995.

735 Guenther, A. B., Zimmerman, P. R., and Harley, P. C.: Isoprene and monoterpene emission rate

736 variability: model evaluations and sensitivity analyses, J. Geophys. Res., 98, 12,609-612,617, 1993.

737 Guo, H., Cheng, H. R., Ling, Z. H., Louie, P. K., and Ayoko, G. A.: Which emission sources are

738 responsible for the volatile organic compounds in the atmosphere of Pearl River Delta?, J. Hazard.

739 Mater., 188, 116-124, 10.1016/j.jhazmat.2011.01.081, 2011.

740 Guo, H., Ling, Z. H., Cheng, H. R., Simpson, I. J., Lyu, X. P., Wang, X. M., Shao, M., Lu, H. X.,

741 Ayoko, G., Zhang, Y. L., Saunders, S. M., Lam, S. H. M., Wang, J. L., and Blake, D. R.:

742 Tropospheric volatile organic compounds in China, Sci. Total Environ., 574, 1021-1043,

743 10.1016/j.scitotenv.2016.09.116, 2017.

744 Guo, S., Tan, J., Duan, J., Ma, Y., Yang, F., He, K., and Hao, J.: Characteristics of atmospheric

745 non-methane hydrocarbons during haze episode in Beijing, China, Environ. Monit. Assess., 184,

746 7235-7246, 10.1007/s10661-011-2493-9, 2012.

747 Haagen-Smit, A. T.: Chemistry and physiology of Los Angeles smog, J. Ind. Eng. Chem., 44,

748 1342-1346, 1952.

749 Hanna, S. R., Moore, G. E., and Fernau, M.: Evaluation of photochemical grid models (UAM-IV,

750 UAM-V, and the ROM/UAM-IV couple) using data from the Lake Michigan Ozone Study (LMOS)

751 Atmos. Environ., 30, 3265-3279, 1996.

752 Hidy, G. M., and Blanchard, C. L.: Precursor reductions and ground-level ozone in the Continental

753 United States, J. Air & Waste Manage. Assoc., 65, 1261-1282, 10.1080/10962247.2015.1079564,

754 2015.

755 Ho, K. F., Lee, S. C., Ho, W. K., Blake, D. R., Cheng, Y., Li, Y. S., Ho, S. S. H., Fung, K., Louie, P.

756 K. K., and Park, D.: Vehicular emission of volatile organic compounds (VOCs) from a tunnel study

757 in Hong Kong, Atmos. Chem. Phys., 9, 7491–7504, 2009.

758 Hopke, P. K., Barrie, L. A., Li, S.-M., M.-D.Cheng, C.Li, and Xie, Y.: Possible sources and

759 preferred pathways for biogenic and non-sea-salt sulfur for the high Arctic, J. Geophys.

760 Res.-Atmos., 100, 16,595-516,603, 1995.

761 Huang, Y., Ling, Z. H., Lee, S. C., Ho, S. S. H., Cao, J. J., Blake, D. R., Cheng, Y., Lai, S. C., Ho,

762 K. F., Gao, Y., Cui, L., and Louie, P. K. K.: Characterization of volatile organic compounds at a

763 roadside environment in Hong Kong: An investigation of influences after air pollution control

764 strategies, Atmos. Environ., 122, 809-818, 10.1016/j.atmosenv.2015.09.036, 2015.

765 Jia, C., Mao, X., Huang, T., Liang, X., Wang, Y., Shen, Y., Jiang, W., Wang, H., Bai, Z., Ma, M.,

766 Yu, Z., Ma, J., and Gao, H.: Non-methane hydrocarbons (NMHCs) and their contribution to ozone

767 formation potential in a petrochemical industrialized city, Northwest China, Atmos. Res., 169,

768 225-236, 10.1016/j.atmosres.2015.10.006, 2016.

769 Jin, X., and Holloway, T.: Spatial and temporal variability of ozone sensitivity over China observed

770 from the Ozone Monitoring Instrument, J. Geophys. Res.-Atmos., 120, 7229-7246,

771 10.1002/2015jd023250, 2015.

772 Jobson, B. T., Berkowitz, C. M., Kuster, W. C., Goldan, P. D., Williams, E. J., Fesenfeld, F. C.,

773 Apel, E. C., Karl, T., Lonneman, W. A., and Riemer, D.: Hydrocarbon source signatures in Houston,

774 Texas: Influence of the petrochemical industry, J. Geophys. Res.-Atmos., 109,

775 10.1029/2004jd004887, 2004.

776 Lau, A. K., Yuan, Z., Yu, J. Z., and Louie, P. K.: Source apportionment of ambient volatile organic

777 compounds in Hong Kong, Sci. Total Environ., 408, 4138-4149, 10.1016/j.scitotenv.2010.05.025,

778 2010.

779 Li, B., Ho, S. S. H., Xue, Y., Huang, Y., Wang, L., Cheng, Y., Dai, W., Zhong, H., Cao, J., and Lee,

780 S.: Characterizations of volatile organic compounds (VOCs) from vehicular emissions at roadside

781 environment: The first comprehensive study in Northwestern China, Atmos. Environ., 161, 1-12,

782 10.1016/j.atmosenv.2017.04.029, 2017a.

783 Li, K., Chen, L., Ying, F., White, S. J., Jang, C., Wu, X., Gao, X., Hong, S., Shen, J., Azzi, M., and

784 Cen, K.: Meteorological and chemical impacts on ozone formation: A case study in Hangzhou,

785 China, Atmos. Res., 10.1016/j.atmosres.2017.06.003, 2017b.

786   Li, L., and Wang, X.: Seasonal and diurnal variations of atmospheric non-methane hydrocarbons in

787   Guangzhou, China, Inter. J. .Env. Res. Pub. Heal., 9, 1859-1873, 10.3390/ijerph9051859, 2012.

788   Li, L., Chen, Y., Zeng, L., Shao, M., Xie, S., Chen, W., Lu, S., Wu, Y., and Cao, W.: Biomass

789   burning contribution to ambient volatile organic compounds (VOCs) in the Chengdu–Chongqing

790   Region (CCR), China, Atmos. Environ., 99, 403-410, 10.1016/j.atmosenv.2014.09.067, 2014.

791   Li, Q., Zhang, L., Wang, T., Wang, Z., Fu, X., and Zhang, Q.: "New" Reactive Nitrogen Chemistry

792   Reshapes the Relationship of Ozone to Its Precursors, Environ. Sci. Technol., 52, 2810-2818,

793   10.1021/acs.est.7b05771, 2018.

794   Lin, X., Traner, M., and Liu, S. C.: On the Nonlinearity of the Tropospheric Ozone Production, J.

795   Geophys. Res.-Atmos., 93, 15879-15888, 1998.

796   Liu, B., Liang, D., Yang, J., Dai, Q., Bi, X., Feng, Y., Yuan, J., Xiao, Z., Zhang, Y., and Xu, H.:

797   Characterization and source apportionment of volatile organic compounds based on 1-year of

798   observational data in Tianjin, China, Environ. Pollut., 218, 757-769, 10.1016/j.envpol.2016.07.072,

799   2016.

800   Liu, H., Liu, S., Xue, B., Lv, Z., Meng, Z., Yang, X., Xue, T., Yu, Q., and He, K.: Ground-level

801   ozone pollution and its health impacts in China, Atmos. Environ., 173, 223-230,

802   10.1016/j.atmosenv.2017.11.014, 2018.

803   Liu, Y., Shao, M., Fu, L., Lu, S., Zeng, L., and Tang, D.: Source profiles of volatile organic

804   compounds (VOCs) measured in China: Part I, Atmos. Environ., 42, 6247-6260,

805   10.1016/j.atmosenv.2008.01.070, 2008.

806   Liu, Y., Yuan, B., Li, X., Shao, M., Lu, S., Li, Y., Chang, C. C., Wang, Z., Hu, W., Huang, X., He,

807   L., Zeng, L., Hu, M., and Zhu, T.: Impact of pollution controls in Beijing on atmospheric

808   oxygenated volatile organic compounds (OVOCs) during the 2008 Olympic Games: observation

809   and modeling implications, Atmos. Chem. Phys., 15, 3045-3062, 10.5194/acp-15-3045-2015, 2015.

810   Louie, P. K. K., Ho, J. W. K., Tsang, R. C. W., Blake, D. R., Lau, A. K. H., Yu, J. Z., Yuan, Z.,

811   Wang, X., Shao, M., and Zhong, L.: VOCs and OVOCs distribution and control policy implications

812   in Pearl River Delta region, China, Atmos. Environ., 76, 125-135, 10.1016/j.atmosenv.2012.08.058,

813   2013.

814 Luecken, D. J., Napelenok, S. L., Strum, M., Scheffe, R., and Phillips, S.: Sensitivity of Ambient

815 Atmospheric Formaldehyde and Ozone to Precursor Species and Source Types Across the United

816 States, Environ. Sci. Technol., 52, 4668-4675, 10.1021/acs.est.7b05509, 2018.

817 Lyu, X. P., Chen, N., Guo, H., Zhang, W. H., Wang, N., Wang, Y., and Liu, M.: Ambient volatile

818 organic compounds and their effect on ozone production in Wuhan, central China, Sci. Total

819 Environ., 541, 200-209, 10.1016/j.scitotenv.2015.09.093, 2016.

820 Malley, C. S., Braban, C. F., Dumitrean, P., Cape, J. N., and Heal, M. R.: The impact of speciated

821 VOCs on regional ozone increment derived from measurements at the UK EMEP supersites

822 between 1999 and 2012, Atmos. Chem. Phys., 15, 8361-8380, 10.5194/acp-15-8361-2015, 2015.

823 McGaughey, G. R., Desai, N. R., Allen, D. T., Seila, R. L., Lonneman, W. A., Fraser, M. P., Harley,

824 R. A., Pollack, A. K., Ivy, J. M., and Price, J. H.: Analysis of motor vehicle emissions in a Houston

825 tunnel during the Texas Air Quality Study 2000, Atmos. Environ., 38, 3363-3372,

826 10.1016/j.atmosenv.2004.03.006, 2004.

827 Na, K., Kim, Y. P., Moon, K.-C., Moon, I., and Fung, K.: Concentrations of volatile organic

828 compounds in an industrial area of Korea, Atmos. Environ., 35, 2747-2756, 2001.

829 Nagashima, T., Sudo, K., Akimoto, H., Kurokawa, J., and Ohara, T.: Long-term change in the

830 source contribution to surface ozone over Japan, Atmos. Chem. Phys., 17, 8231-8246,

831 10.5194/acp-17-8231-2017, 2017.

832 Oliver, K. D., Adams, J. R., JR, E. H. D., Mcclenny, W. A., Yoong, M. J., and Pardee, M. A.:

833 Technique for monitoring ozone precursor hydrocarbons in air at photochemical assessment

834 monitoring stations: sorbent preconcentration, closed-cycle cooler cryofocusing, and GC-FID

835 analysis, Atmos. Environ., 30, 2751-2757, 1996.

836 Ou, J., Zheng, J., Li, R., Huang, X., Zhong, Z., Zhong, L., and Lin, H.: Speciated OVOC and VOC

837 emission inventories and their implications for reactivity-based ozone control strategy in the Pearl

838 River Delta region, China, Sci. Total Environ., 530-531, 393-402, 10.1016/j.scitotenv.2015.05.062,

839 2015.

840 Ou, J., Yuan, Z., Zheng, J., Huang, Z., Shao, M., Li, Z., Huang, X., Guo, H., and Louie, P. K.:

841 Ambient Ozone Control in a Photochemically Active Region: Short-Term Despiking or Long-Term

842 Attainment?, Environ. Sci. Technol., 50, 5720-5728, 10.1021/acs.est.6b00345, 2016.

843 Polissar, A. V., Hopke, P. K., Paatero, P., Kaufmann, Y. J., Hall, D. K., Bodhaine, B. A., Dutton, E.

844 G., and Harris, J. M.: The aerosol at Barrow, Alaska: long-term trends and source locations, Atmos.

845 Environ., 33, 2441-2458, 1999.

846 Pollack, I. B., Ryerson, T. B., Trainer, M., Neuman, J. A., Roberts, J. M., and Parrish, D. D.:

847 Trends in ozone, its precursors, and related secondary oxidation products in Los Angeles,

848 California: A synthesis of measurements from 1960 to 2010, J. Geophys. Res.-Atmos., 118,

849 5893-5911, 10.1002/jgrd.50472, 2013.

850 Raysoni, A. U., Stock, T. H., Sarnat, J. A., Chavez, M. C., Sarnat, S. E., Montoya, T., Holguin, F.,

851 and Li, W. W.: Evaluation of VOC concentrations in indoor and outdoor microenvironments at

852 near-road schools, Environ. Pollut., 231, 681-693, 10.1016/j.envpol.2017.08.065, 2017.

853 Russo, R. S., Zhou, Y., White, M. L., Mao, H., Talbot, R., and Sive, B. C.: Multi-year (2004–2008)

854 record of nonmethane hydrocarbons and halocarbons in New England: seasonal variations and

855 regional sources, Atmos. Chem. Phys., 10, 4909-4929, 10.5194/acp-10-4909-2010, 2010.

856 Shao, M., Lu, S., Liu, Y., Xie, X., Chang, C., Huang, S., and Chen, Z.: Volatile organic compounds

857 measured in summer in Beijing and their role in ground‐level ozone formation, J. Geophys.

858 Res.-Atmos., 114, 10.1029/2008jd010863, 2009.

859 Shao, M., Wang, B., Lu, S., Yuan, B., and Wang, M.: Effects of Beijing Olympics Control

860 Measures on Reducing Reactive Hydrocarbon Species, Environ. Sci. Technol., 45, 514-519, 2011.

861 Shao, P., An, J., Xin, J., Wu, F., Wang, J., Ji, D., and Wang, Y.: Source apportionment of VOCs

862 and the contribution to photochemical ozone formation during summer in the typical industrial area

863 in the Yangtze River Delta, China, Atmos. Res., 176-177, 64-74, 10.1016/j.atmosres.2016.02.015,

864 2016.

865 Shen, F., Ge, X., Hu, J., Nie, D., Tian, L., and Chen, M.: Air pollution characteristics and health

866 risks in Henan Province, China, Environ. Res., 156, 625-634, 10.1016/j.envres.2017.04.026, 2017.

867 Shiu, C.-J., Liu, S. C., Chang, C.-C., Chen, J.-P., Chou, C. C. K., Lin, C.-Y., and Young, C.-Y.:

868 Photochemical production of ozone and control strategy for Southern Taiwan, Atmos. Environ., 41,

869 9324-9340, 10.1016/j.atmosenv.2007.09.014, 2007.

870 Sillman, S.: The relation between ozone, NOx and hydrocarbons in urban and polluted rural

871 environments, Atmos. Environ., 33, 1821-1845, 1999.

872 Streets, D. G., Fu, J. S., Jang, C. J., Hao, J., He, K., Tang, X., Zhang, Y., Wang, Z., Li, Z., Zhang,

873 Q., Wang, L., Wang, B., and Yu, C.: Air quality during the 2008 Beijing Olympic Games, Atmos.

874 Environ., 41, 480-492, 10.1016/j.atmosenv.2006.08.046, 2007.

875 Sun, J., Wu, F., Hu, B., Tang, G., Zhang, J., and Wang, Y.: VOC characteristics, emissions and

876 contributions to SOA formation during hazy episodes, Atmos. Environ., 141, 560-570,

877 10.1016/j.atmosenv.2016.06.060, 2016.

878 Tang, J. H., Chan, L. Y., Chan, C. Y., Li, Y. S., Chang, C. C., Liu, S. C., Wu, D., and Li, Y. D.:

879 Characteristics and diurnal variations of NMHCs at urban, suburban, and rural sites in the Pearl

880 River Delta and a remote site in South China, Atmos. Environ., 41, 8620-8632,

881 10.1016/j.atmosenv.2007.07.029, 2007.

882 Tsai, S. M., Zhang, J. J., Smith, K. R., Ma, Y., Rasmussen, R. A., and Khalil, M. A. K.:

883 Characterization of Non-methane Hydrocarbons Emitted from Various Cookstoves Used in China,

884 Environ. Sci. Technol., 37, 2869-2877, 2003.

885 US EPA: Compendium Method TO-15: Determination of volatile organic compounds in air

886 collected in specially prepared canisters and analyzed by gas chromatography/mass spectrometry,

887 1999.

888 US EPA, National air pollutant emission trends 1900–1998, Off. Air Qual. Plann. Stand., Research

889 Triangle Park, N. C, Rep. EPA 454/R-00-002, 2000.

890 US   EPA: Photochemical   Assessment   Monitoring   Stations   (PAMS),   available   at:

891 https://www3.epa.gov/ttnamti1/pamsmain.html, (last access: 03 December 2018), 1990.

892 Wang, H.-l., Jing, S.-a., Lou, S.-r., Hu, Q.-y., Li, L., Tao, S.-k., Huang, C., Qiao, L.-p., and Chen,

893 C.-h.: Volatile organic compounds (VOCs) source profiles of on-road vehicle emissions in China,

894 Sci. Total Environ., 607-608, 253-261, 10.1016/j.scitotenv.2017.07.001, 2017a.

895 Wang, H., Qiao, Y., Chen, C., Lu, J., Qiao, L., and Lou, S.: Source Profiles and Chemical

896 Reactivity of Volatile Organic Compounds from Solvent Use in Shanghai, China, Aerosol Air Qual.

897 Res., 10.4209/aaqr.2013.03.0064, 2014.

898 Wang, M., Shao, M., Lu, S.-H., Yang, Y.-D., and Chen, W.-T.: Evidence of coal combustion

899 contribution to ambient VOCs during winter in Beijing, Chin. Chem. Lett., 24, 829-832,

900 10.1016/j.cclet.2013.05.029, 2013.

Wang, M., Shao, M., Chen, W., Lu, S., Liu, Y., Yuan, B., Zhang, Q., Zhang, Q., Chang, C. C., Wang, B., Zeng, L., Hu, M., Yang, Y., and Li, Y.: Trends of non-methane hydrocarbons (NMHC) emissions in Beijing during 2002–2013, Atmos. Chem. Phys., 15, 1489-1502, 10.5194/acp-15-1489-2015, 2015.

Wang, Q., Li, S., Dong, M., Li, W., Gao, X., Ye, R., and Zhang, D.: VOCs emission characteristics and priority control analysis based on VOCs emission inventories and ozone formation potentials in Zhoushan, Atmos. Environ., 182, 234-241, 2018.

Wang, T., Xue, L., Brimblecombe, P., Lam, Y. F., Li, L., and Zhang, L.: Ozone pollution in China: A review of concentrations, meteorological influences, chemical precursors, and effects, Sci. Total Environ., 575, 1582-1596, 10.1016/j.scitotenv.2016.10.081, 2017b.

Wang, X.-m., Sheng, G.-y., Fu, J.-m., Chan, C.-y., Lee, S.-C., Chan, L. Y., and Wang, Z.-s.: Urban roadside aromatic hydrocarbons in three cities of the Pearl River Delta, People's Republic of China, Atmos. Environ., 36, 5141–5148, 2002.

Wei, W., Cheng, S., Li, G., Wang, G., and Wang, H.: Characteristics of ozone and ozone precursors (VOCs and NOx) around a petroleum refinery in Beijing, China, J. Environ. Sci.-China, 26, 332-342, 10.1016/s1001-0742(13)60412-x, 2014.

Wu, R., and Xie, S.: Spatial Distribution of Ozone Formation in China Derived from Emissions of Speciated Volatile Organic Compounds, Environ. Sci. Technol., 51, 2574-2583, 10.1021/acs.est.6b03634, 2017.

Xue, Y., Ho, S. S. H., Huang, Y., Li, B., Wang, L., Dai, W., Cao, J., and Lee, S.: Source apportionment of VOCs and their impacts on surface ozone in an industry city of Baoji, Northwestern China, Sci. Rep., 7, 9979, 10.1038/s41598-017-10631-4, 2017.

Yan, Y., Peng, L., Li, R., Li, Y., Li, L., and Bai, H.: Concentration, ozone formation potential and source analysis of volatile organic compounds (VOCs) in a thermal power station centralized area: A study in Shuozhou, China, Environ. Pollut., 223, 295-304, 10.1016/j.envpol.2017.01.026, 2017.

Yuan, B., Shao, M., de Gouw, J., Parrish, D. D., Lu, S., Wang, M., Zeng, L., Zhang, Q., Song, Y., Zhang, J., and Hu, M.: Volatile organic compounds (VOCs) in urban air: How chemistry affects the interpretation of positive matrix factorization (PMF) analysis, J. Geophys. Res.-Atmos., 117, n/a-n/a, 10.1029/2012jd018236, 2012.

930   Zhang, Z., Wang, X., Zhang, Y., Lu, S., Huang, Z., Huang, X., and Wang, Y.: Ambient air benzene

931   at background sites in China's most developed coastal regions: exposure levels, source implications

932   and health risks, Sci. Total Environ., 511, 792-800, 10.1016/j.scitotenv.2015.01.003, 2015.

933   Zhu, Y., Yang, L., Chen, J., Wang, X., Xue, L., Sui, X., Wen, L., Xu, C., Yao, L., Zhang, J., Shao,

934   M., Lu, S., and Wang, W.: Characteristics of ambient volatile organic compounds and the influence

935   f biomass burning at a rural site in Northern China during summer 2013, Atmos. Environ., 124,

936   156-165, 10.1016/j.atmosenv.2015.08.097, 2016.

937

938

939